

General Disclaimer

One or more of the Following Statements may affect this Document

- This document has been reproduced from the best copy furnished by the organizational source. It is being released in the interest of making available as much information as possible.
- This document may contain data, which exceeds the sheet parameters. It was furnished in this condition by the organizational source and is the best copy available.
- This document may contain tone-on-tone or color graphs, charts and/or pictures, which have been reproduced in black and white.
- This document is paginated as submitted by the original source.
- Portions of this document are not fully legible due to the historical nature of some of the material. However, it is the best reproduction available from the original submission.



The Ohio State University

ADAPTIVE ANTENNA ARRAYS FOR SATELLITE COMMUNICATIONS -
DESIGN AND TESTING

Inder J. Gupta
William G. Swarner
Eric K. Walton

The Ohio State University
ElectroScience Laboratory

Department of Electrical Engineering
Columbus, Ohio 43212

(NASA-CR-176162) ADAPTIVE ANTENNA ARRAYS
FOR SATELLITE COMMUNICATIONS: DESIGN AND
TESTING (Ohio State Univ., Columbus.) 116 p
HC AG6/MF B1 CSCL 20A

N85-34329

Unclas
22197

33/32



Technical Report 716111-3
Grant No. NAG3-536
September 1985

National Aeronautics and Space Administration
Lewis Research Center
21000 Brookpark Road
Cleveland, Ohio 44135

REPORT DOCUMENTATION PAGE	1. REPORT NO.	2.	3. Recipient's Accession No.
4. Title and Subtitle ADAPTIVE ANTENNA ARRAYS FOR SATELLITE COMMUNICATIONS - DESIGN AND TESTING			5. Report Date September 1985
7. Author(s) Inder J. Gupta, William G. Swarner and Eric K. Walton			6. 8. Performing Organization Rept. No. ESL 716111-3
9. Performing Organization Name and Address The Ohio State University ElectroScience Laboratory Department of Electrical Engineering Columbus, Ohio 43212			10. Project/Task/Work Unit No. 11. Contract(C) or Grant(G) No. (C) (G) NAG-536
12. Sponsoring Organization Name and Address National Aeronautics and Space Administration Lewis Research Center 21000 Brookpark Road Cleveland, Ohio 44135			13. Type of Report & Period Covered Technical Report
15. Supplementary Notes			
<p>16. Abstract (Limit 200 words)</p> <p>In satellite communication systems where the interference is caused by transmission from adjacent satellites or earth stations whose signals inadvertently enter the receiving system, conventional adaptive antenna arrays may not provide sufficient interference suppression. The reason for the lack of interference suppression is that the interference signals are very weak. To overcome this difficulty and to achieve the desired interference suppression, the auxiliary elements of adaptive arrays should be directive and steered in the general direction of the interfering signals. The feedback loops controlling the array weights should also be modified. In the modified feedback loops, the noise level in the feedback loops is reduced by reducing the correlation between the noise components of the two inputs to the correlators in the feedback loops. When two separate antennas are used with each feedback loop to decorrelate noise, the antennas should be located such that the phase of the interfering signal in the two antennas is the same while the noise in them is uncorrelated. Thus, the antenna patterns and spatial distribution of the auxiliary antennas are quite important and should be carefully selected. In this work, the selection and spatial distribution of auxiliary elements is discussed when the main antenna is a center-fed reflector antenna. It is shown that offset feeds of the reflector antenna can be used as auxiliary elements of an adaptive array to suppress weak interfering signals. An experimental system is designed to verify the theoretical analysis. The details of the experimental systems are presented. Various tests proposed to verify the</p>			
17. Document Analysis a. Descriptors analytical work are also discussed.			
<p>b. Identifiers/Open-Ended Terms</p> <p>c. COSATI Field/Group</p>			
18. Availability Statement		19. Security Class (This Report) Unclassified	21. No. of Pages 108
		20. Security Class (This Page) Unclassified	22. Price

TABLE OF CONTENTS

CHAPTER		PAGE
	LIST OF FIGURES	iii
I	INTRODUCTION	1
II	THE MAIN ANTENNA AND ITS RADIATION CHARACTERISTICS	5
III	DEFOCUSED FEEDS AS AUXILIARY ELEMENTS	20
	A. INTRODUCTION	20
	B. FULLY ADAPTIVE ANTENNA ARRAY	22
	C. THE PERFORMANCE OF A SIDELOBE CANCELLER	36
	D. SIDELOBE CANCELLER WITH MODIFIED FEEDBACK LOOPS	45
	E. NOISE DECORRELATION USING OFFSET FEEDS	52
	F. TWO INTERFERING SIGNALS	62
IV	EXPERIMENTAL SYSTEM	76
	A. INTRODUCTION	76
	B. SIGNAL SCENARIOS	76
	C. ANTENNA CONFIGURATION	79
	D. ARRAY SIMULATOR	81
	E. ARRAY PROCESSOR	86
	F. EXPERIMENTAL VERIFICATION AND TESTING	91
V	SUMMARY AND FUTURE WORK	94
	REFERENCES	96
	APPENDIX A	97

LIST OF FIGURES

FIGURE		PAGE
1	Center-fed circular reflector.	6
2	Center-fed circular reflector.	8
3	Analytic feed pattern with linear taper region.	9
4	Feed pattern in y-z plane.	11
5	Radiation pattern of the antenna in y-z plane when the feed is at the focus.	12
6	Radiation pattern of the antenna in y-z plane when the feed is $(0., \lambda, 0.)$ away from the focus.	13
7	Radiation pattern of the antenna in y-z plane when the feed is $(0., 2\lambda, 0.)$ away from the focus.	15
8	Radiation pattern of the antenna in y-z plane when the feed is $(0., 3\lambda, 0.)$ away from the focus.	16
9	Radiation pattern of the antenna in y-z plane when the feed is $(0., -2\lambda, 0.)$ away from the focus.	17
10	Radiation pattern of the antenna in y-z plane when the feed is $(0., -3\lambda, 0.)$ away from the focus.	18
11	Source distribution in a satellite communication system.	21
12	INR at the output of the feed at the focus vs. interfering signal direction. INR (isotropic) = -30 dB.	23
13	Output INR of a fully adaptive array vs. interfering signal direction. One offset feed at $(0., 2\lambda, 0.)$, $G/\alpha = 100$. INR (isotropic) = -30 dB.	24
14	Fully adaptive array with one offset feed (a) and a typical feedback loop (b).	25

FIGURE		PAGE
15	Output SINR of a fully adaptive array vs. interfering signal direction. One offset feed at $(0., 2\lambda, 0.)$, INR (isotropic) = -30 dB, $G/\alpha = 100$.	26
16	Output INR of a fully adaptive array vs. interfering signal direction. One offset feed at $(0., 3\lambda, 0.)$, INR (isotropic) = -30 dB, $G/\alpha = 100$.	28
17	Output SINR of a fully adaptive array vs. interfering signal direction. One offset feed at $(0., 3\lambda, 0.)$, INR (isotropic) = -30 dB, $G/\alpha = 100$.	29
18	Output INR of a fully adaptive array vs. interfering signal direction. Two offset feeds at $(0., 2\lambda, 0.)$ and $(0., 3\lambda, 0.)$, respectively. INR (isotropic) = -30 dB, $G/\alpha = 100$.	30
19	INR at the output of the feed at the focus vs. interfering signal direction. INR (isotropic) = -40 dB.	32
20	Output INR of a fully adaptive array vs. the interfering signal direction. One offset feed at $(0., 2\lambda, 0.)$, INR (isotropic) = -40 dB, $G/\alpha = 100$.	33
21	Output INR of a fully adaptive array vs. the interfering signal direction. Two offset feeds at $(0., 2\lambda, 0.)$ and $(0., 3\lambda, 0.)$, respectively. INR (isotropic) = -30 dB, $G/\alpha = 100$.	35
22	Sidelobe canceller with one offset feed.	37
23	Output INR of a sidelobe canceller vs. the interfering signal direction. One offset feed at $(0., 2\lambda, 0.)$, INR (isotropic) = -30 dB, $G/\alpha = 100$.	38
24	Output INR of a sidelobe canceller vs. the interfering signal direction. One offset feed at $(0., 3\lambda, 0.)$, INR (isotropic) = -30 dB, $G/\alpha = 100$.	39
25	Output SINR of a sidelobe canceller vs. the interfering signal direction. One offset feed at $(0., 2\lambda, 0.)$, INR (isotropic) = -30 dB, $G/\alpha = 100$.	41

FIGURE		PAGE
26	Output SINR of a sidelobe canceller vs. the interfering signal direction. One offset feed at $(0., 3\lambda, 0.)$, INR (isotropic) = -30 dB, $G/\alpha = 100$.	42
27	Output INR of a sidelobe canceller vs. the interfering signal direction. Two offset feeds at $(0., 2\lambda, 0.)$ and $(0., 3\lambda, 0.)$, respectively. INR (isotropic) = -30 dB, $G/\alpha = 100$.	43
28	Output INR of a sidelobe canceller vs. the interfering signal direction. Two offset feeds at $(0., 2\lambda, 0.)$ and $(0., 3\lambda, 0.)$, respectively. INR (isotropic) = -40 dB, $G/\alpha = 100$.	44
29	Output INR of a sidelobe canceller vs. the interfering signal direction. One offset feed at $(0., 2\lambda, 0.)$ and modified feedback loop is used. INR (isotropic) = -30 dB, $G/\alpha = 100$.	47
30	Output INR of a sidelobe canceller vs. the interfering signal direction. INR (isotropic) = -40 dB. Other parameters are the same as in Figure 29.	49
31	Feedback loop with two amplifiers.	50
32	Feedback loop with two antennas.	51
33	Phase of the radiated field in the yz plane when the feed is $(0.5\lambda, 2\lambda, 0.)$ away from the focus.	54
34	Phase of the radiated field in the yz plane when the feed is $(-0.5\lambda, 2\lambda, 0.)$ away from the focus.	55
35	Output INR of a sidelobe canceller with one modified feedback loop vs. the interfering signal direction. A pair of offset feeds at $(\pm 0.5\lambda, 2\lambda, 0.)$, INR (isotropic) = -30 dB, $G/\alpha = 100$.	57
36	Radiation pattern of the antenna in yz plane when the feed is $(0.5\lambda, 2\lambda, 0.)$ away from the focus.	59
37	Radiation pattern of the antenna in yz plane when the feed is $(-0.5\lambda, 2\lambda, 0.)$ away from the focus.	60

FIGURE		PAGE
38	Output INR of a sidelobe canceller with one modified feedback loop vs. the interfering signal direction. INR (isotropic) = -40 dB. Other parameters are the same as in Figure 35.	61
39	INR at the output of the feed at the focus vs. swept interference signal direction. Two interfering signals. $\theta_{j1} = 5.5^\circ$, INR (isotropic) for each interfering signal = -30 dB.	63
40	Output INR of a sidelobe canceller vs. the swept interference signal direction. One offset feed at (0., -3λ , 0.). Two interfering signals $\theta_{j1} = 5.5^\circ$, INR (isotropic) for each interfering signal = -30 dB, $G/\alpha = 100$.	65
41	Output INR of a sidelobe canceller vs. the swept interference signal direction. Two offset feeds at (0., -3λ , 0.) and (0., 2λ , 0.), respectively. Other parameters are the same as in Figure 40.	67
42	Output SINR of a sidelobe canceller vs. the swept interference signal direction. All parameters are the same as in Figure 41.	68
43	INR at the output of the feed at the focus vs. the swept interference signal direction. Two interfering signals. $\theta_{j1} = -5.5^\circ$, INR (isotropic) for each interfering signal = -30 dB.	70
44	Output INR of a sidelobe canceller vs. the swept interference signal direction. One offset feed at (0., 3λ , 0.). Two interfering signals, $\theta_{j1} = -5.5^\circ$, INR (isotropic) each interfering signal = -30 dB, $G/\alpha = 100$.	71
45	Output INR of a sidelobe canceller vs. the swept interference signal direction. Two offset feeds at (0., 2λ , 0.) and (0., 3λ , 0.). All other parameters are the same as in Figure 42.	72
46	Output SINR of a sidelobe canceller vs. the swept interference signal direction. All parameters are the same as in Figure 45.	74
47	Block diagram of the experimental system.	77

FIGURE		PAGE
48	Distribution of array element. for the experiment.	80
49	Array simulator.	82
50	Detailed description of the array simulator.	84
51	Schematics of a noise source.	85
52	Array processor.	87
53	Detailed description of the array processor.	89
A.1	Noise spectral density S_n .	98
A.2	Spatial distribution of two isotropic antennas.	98
A.3	Noise correlation between two isotropic antennas vs. the separation between antennas. System bandwidth is assumed to be zero, $\Delta f = 0$.	102
A.4	Noise correlation between two isotropic antennas vs. the separation between antennas for various values of system bandwidth.	103
A.5	A linear array of N isotropic antennas.	105
A.6	Noise correlation between two linear arrays of ten isotropic antennas vs. the separation between the two arrays. System bandwidth is assumed to be zero.	107

I. INTRODUCTION

A major problem in satellite communications is the interference caused by transmission from adjacent satellites whose signals inadvertently enter the receiving system and interfere with the communication link. The same problem arises in the earth to satellite part of the link where transmission from nearby ground stations enters the satellite receivers through their antenna sidelobes. The problem has recently become more serious because of the crowding of the geostationary orbit. Indeed this interference prevents the inclusion of additional satellites which could have been allowed if methods to suppress such interference were available. The interference can be suppressed at the originating station, either space or earth, by lowering the sidelobes of the transmitting antenna. Alternatively, the interfering signals may be suppressed at the receiving site.

Under the present grant, a thorough analysis of adaptive antenna arrays [1-5] to provide interference suppression at the receiving site was carried out [6,7]. In the study, the undesired signals are assumed to be located at arbitrary angular separations from the desired signal source. The spectral characteristics and modulations of the desired and undesired signals are similar. The signal-to-noise ratio (SNR) of the desired signal is expected to be 15 dB. The undesired signals are 10-30 dB below the desired signal level. Thus, the undesired signals are significantly weaker than the desired signal and in fact may be several

dB below noise level. Although weak, these signals because of their coherent nature and their similarity to the desired signal, do cause objectionable interference and must be further suppressed by up to 30 dB.

Since the spectral characteristics and modulations of the desired signal and undesired signals are similar, while the desired signal location is known, sidelobe cancellers [1] and steered beam adaptive arrays [2] were used to provide interference protection. However, it was found that the conventional feedback loops used to control the weights of these adaptive arrays were unable to provide the desired interference suppression [6]. The reason for the lack of interference suppression is that in the satellite communication systems under consideration, the interfering signals, as mentioned above, are relatively weak, occasionally even below thermal noise. Under such conditions, the thermal noise becomes the main source of degradation in the output signal-to-interference-plus-noise ratio (SINR) and thus it (thermal noise) dictates the adaptive array weights. The array adjusts its weights to minimize the thermal noise which in turn maximizes the output SINR. However, the interfering signals remain unsuppressed. To overcome this difficulty and to achieve the desired interference suppression, the auxiliary antennas should be directive and be steered in the general direction of the interfering signals [7]. The feedback loops controlling the array weights should also be modified. In the

modified feedback loops, the noise level in the feedback loops is reduced by reducing the correlation between the noise components of the two inputs to the correlators in the feedback loops.

Two techniques to decorrelate the noise in the two inputs to the feedback loop correlators were presented [6]. When the internal thermal noise is the main noise source, two different amplifiers can be used in each feedback loop to decorrelate the noise. In situations where the external noise is significant two separate antennas displaced from each other should be used with each feedback loop. The two antennas should be located such that the phase of the interfering signal in the two antennas is the same while the noise is uncorrelated. Thus, the antenna patterns, particularly gain in the interfering signal direction and the spatial distribution of the auxiliary antennas are quite important and should be carefully selected. In the present work, the selection of the auxiliary antennas is discussed when the main antenna is a center-fed reflector antenna. The auxiliary antennas are selected to provide high gain in the interfering signal direction. A spatial distribution of auxiliary antennas is given to decorrelate noise in the feedback loops.

In the case of a reflector antenna, by moving the feed away from the focus of the reflector, one can steer the beam of the antenna over a wide angular region. Thus, by a proper selection of the feed location, one can steer the main beam in the general direction of an interfering signal and by using an array of feeds, all signals (desired and undesired) can be received with high gain. One can use two offset

feeds, displaced from each other, for each feedback loop to decorrelate the noise in the feedback loop. In this case, noise entering the two feeds arrives from mostly different portions of the observation range and thus assures relatively small noise correlation. It is shown that the two feeds can be located such that the phase of the various signals (desired and undesired) in the two feeds is the same. Thus, all the above mentioned requirements are met and desired interference suppression can be obtained. In this work, the performance of various adaptive arrays is studied when offset feeds of a reflector antenna are used as auxiliary elements.

An experimental system has been designed to demonstrate the capability of an adaptive array to suppress weak interfering signals and to determine the performance limits which can be achieved in practical applications. The experimental system will operate at 70 MHz with a bandwidth of 6 MHz, representing a typical television channel. It is a sidelobe canceller with two auxiliary elements. Modified feedback loops are used to control the weights of the auxiliary channels. A detailed description of the experimental system and various tests which will be executed to verify the analytical work are also presented in this report.

The main antenna used in this work and its radiation characteristics are discussed in section II. The performance of adaptive arrays with offset feeds as auxiliary elements is studied in section III. Details of the experimental system are given in section IV. Section V contains a summary and proposed future work.

II. THE MAIN ANTENNA AND ITS RADIATION CHARACTERISTICS

In this section, the geometry of the main antenna to be used in the adaptive arrays (discussed below) is described and its radiation characteristics are evaluated. The main antenna, shown in Figure 1, is a 4.5 meter center-fed, vertically polarized (along y axis) circular reflector with an F/D ratio of 0.5. The frequency of operation is 4 GHz. At this frequency, the maximum gain of the antenna is 45.5 dB and its half power beam width (HPBW) is approximately 1.9°. Since we plan to use offset feeds of this reflector as auxiliary elements of the adaptive arrays, its radiation pattern for various feed locations were computed. The Ohio State University ElectroScience Laboratory's NEC - Reflector Antenna Code [8,9] was used for this purpose. A description of the code and the radiation patterns of the reflector antenna for various feed locations are given below.

The NEC-Reflector Antenna Code can be used to compute the near-field as well as the far-field of a reflector antenna with a paraboloidal surface. The code utilizes a combination of the Geometrical Theory of Diffraction (GTD) and Aperture Integration (AI) techniques to compute the antenna pattern. Typically, AI is used to compute the far-field main beam and first sidelobes while GTD is used to compute the wide angle sidelobes and backlobes. For near-field calculations, GTD is used for the whole region. The code can be used to

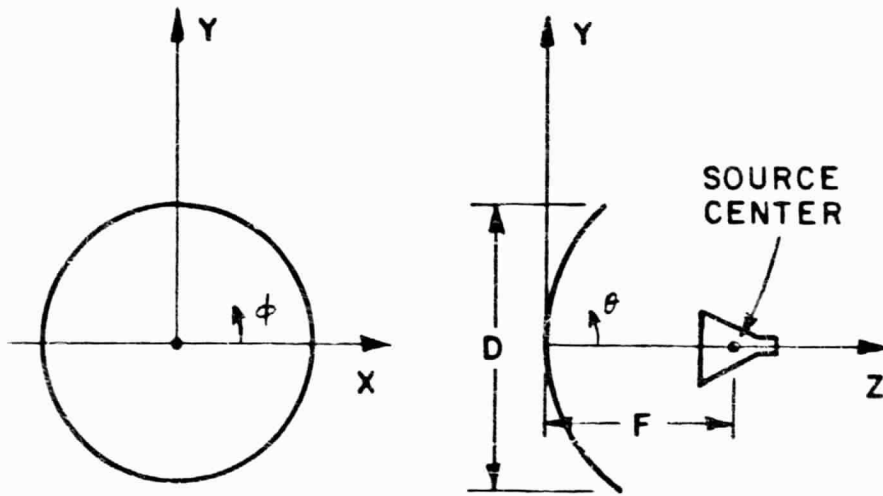


Figure 1. Center-fed circular reflector.

include spillover, feed blockage and scattering from struts etc. and to compute the antenna pattern when the feed is not at the focus (defocussed feed or offset feed) of the reflector.

To compute the antenna pattern, the feed pattern should be specified. In the code, the feed pattern can be specified by piecewise linear feed data or an analytic function. In the case of a horn feed, one need only specify the horn dimensions. The code then computes the feed pattern. The analytic function used to define the feed pattern is

$$F(\psi) = \frac{\exp\left(-A \left(\frac{\psi}{\psi_0}\right)^2\right) \left[\cos^N\left(\frac{\pi\psi}{2\psi_0}\right) + c\right]}{1 + c} \quad (1)$$

where the constants A , ψ_0 , N and c can be controlled for each feed pattern cut ψ_n (Figure 2). The constants A , c and N control the shape of the feed pattern while ψ_0 permits a given pattern shape to be stretched or compressed. For large values of $\frac{\psi}{\psi_0}$ (>1), $F(\psi) \rightarrow \frac{c}{1+c}$. In many cases, this represents a spillover level that is too high for typical feed patterns. Consequently, under certain conditions, a linear taper, as shown in Figure 3, is used for $\psi_L < \psi < 2\psi_L$ where

$$\psi_L = \sqrt{\frac{3}{A}} \psi_0 \quad . \quad (2)$$

The linear taper is found to give reasonable results for $N=1$, $C>0$ and $A>3$. Otherwise, Equation (1) is used for the entire feed pattern.

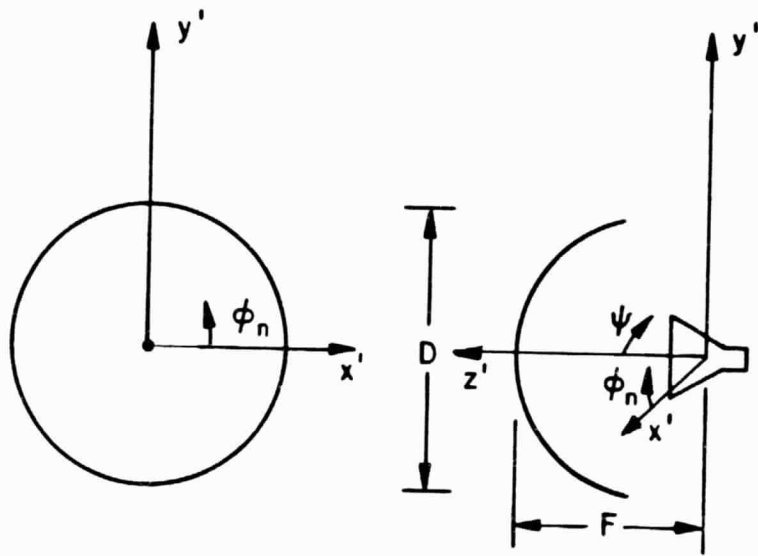


Figure 2. Center-fed circular reflector.

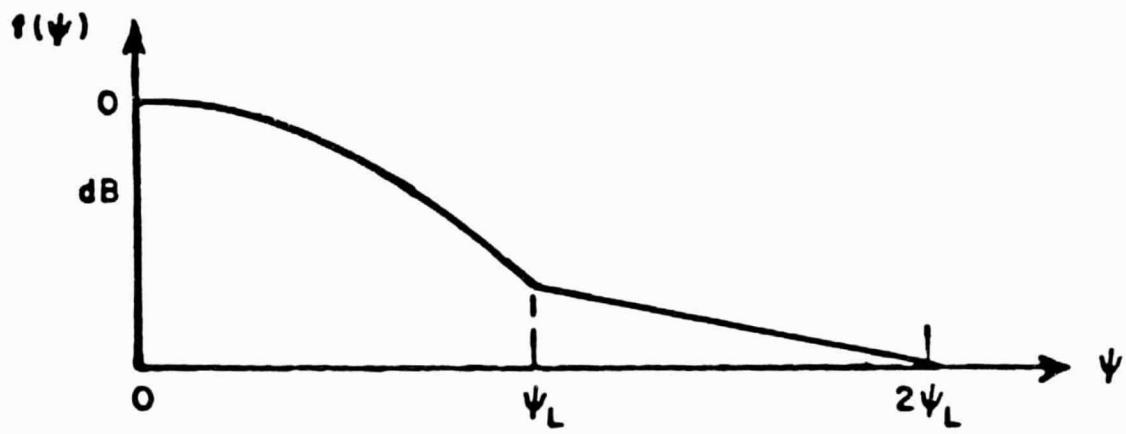


Figure 3. Analytic feed pattern with linear taper region.

In this study, an analytic function is used to specify the feed pattern. The feed pattern is assumed to be circularly symmetric (independent of ϕ_n). The constants A, C and N are chosen to be 3.1, 0, and 1, respectively. This choice leads to a cosine aperture illumination and a small spillover. ψ_0 is chosen such that the edge illumination is -10 dB. Figure 4 shows the feed pattern in the yz plane ($\phi_n = 90^\circ$). Note that the edge illumination is -10 dB (edge angle is 53°) and a linear taper is used for $\psi > \psi_0$, where $\psi_0 = 106^\circ$.

Figure 5 shows the far-field pattern of the reflector in the yz plane ($\phi = 90^\circ$) for $-30^\circ < \theta < 30^\circ$ when the feed is assumed to be at the focus of the reflector. Since we are interested in the general shape of the radiation pattern, aperture blockage and scattering from struts are not included to save computational time. The plot shows the gain of the antenna (over an isotropic radiator) in various directions. The main beam of the antenna is along z axis ($\theta = 0^\circ$) and its gain in this direction is 44.5 dB which is within a dB of the maximum gain of the antenna. The first sidelobe level is 17 dB (27.5 below the main beam). Thus, the SNR of a signal entering the sidelobes will be much lower than that of a signal entering the main beam, even though the EIRP of the two signals is approximately the same.

Figure 6 shows the radiation pattern of the antenna when the feed is moved one wavelength away from the focus along the positive y axis. All other parameters are the same as before. Note that the main beam of

ORIGINAL PAGE IS
OF POOR QUALITY

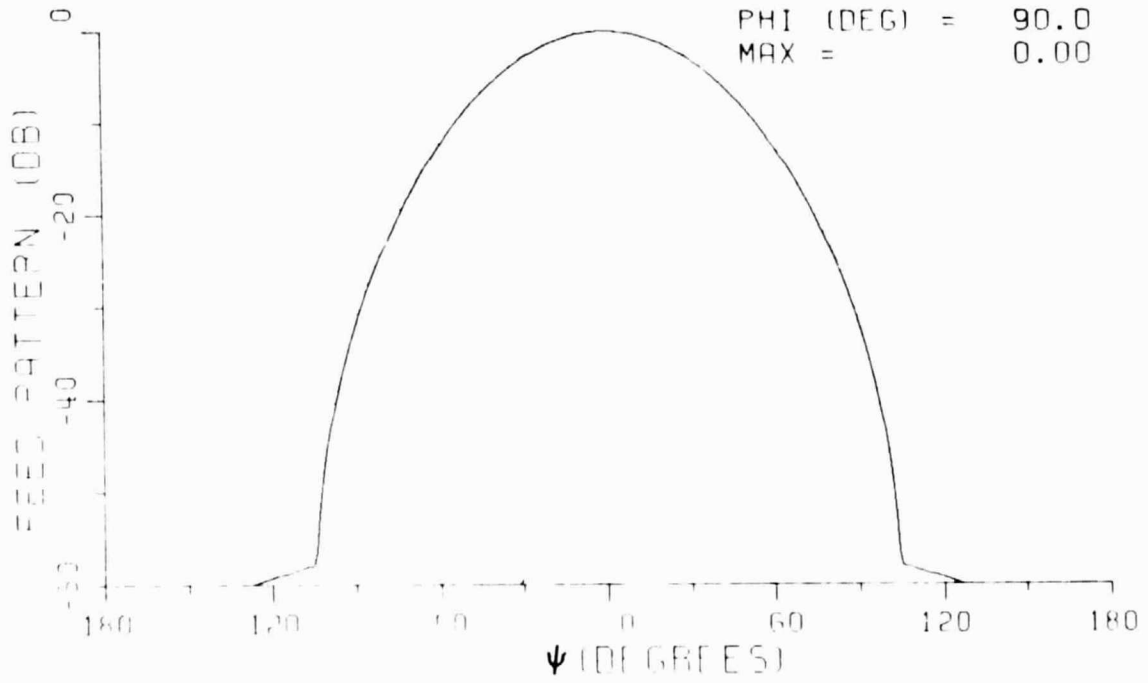


Figure 4. Feed pattern in y-z plane.

ORIGINAL PAGE IS
OF POOR QUALITY

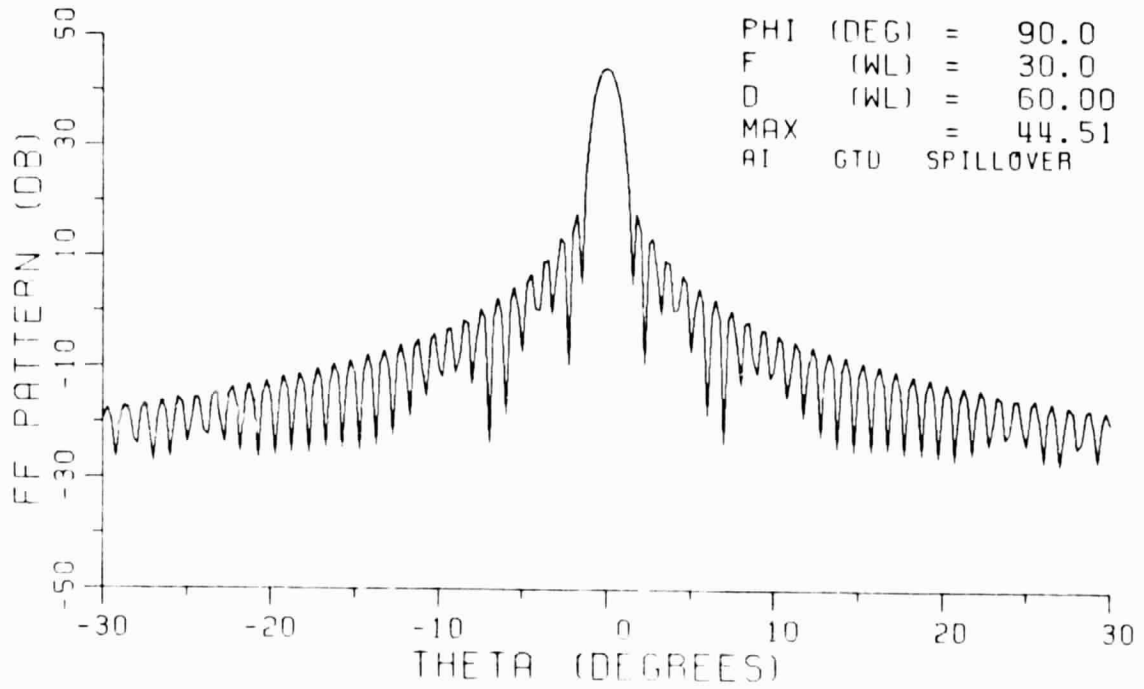


Figure 5. Radiation pattern of the antenna in y-z plane when the feed is at the focus.

ORIGINAL PAGE IS
OF POOR QUALITY

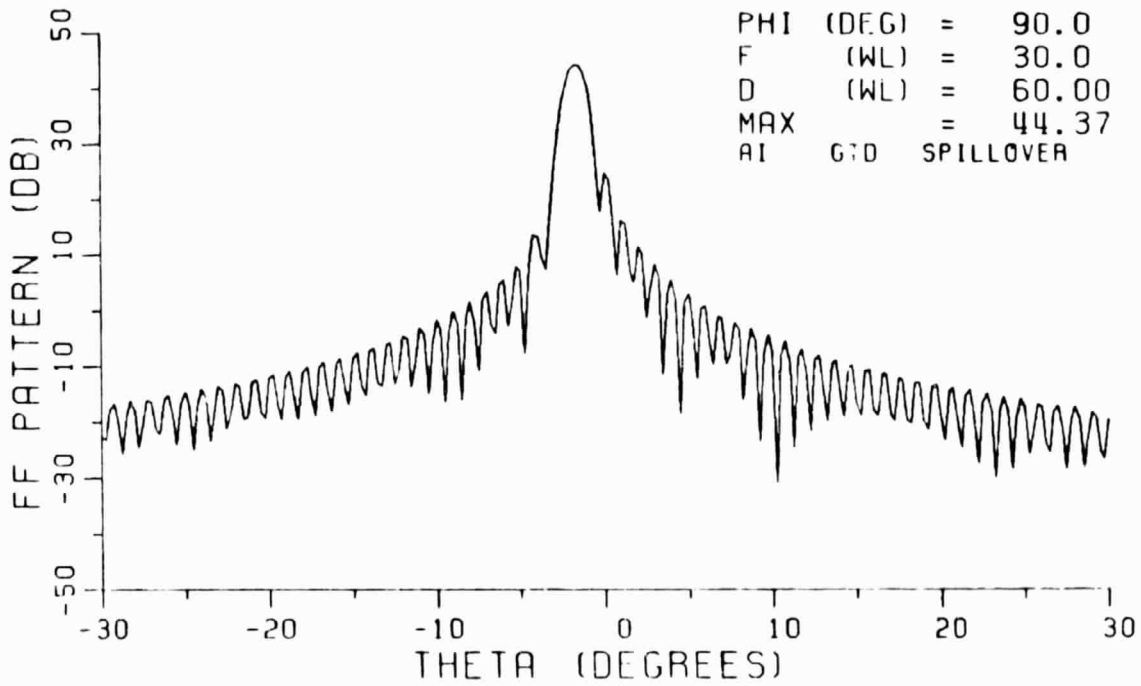


Figure 6. Radiation pattern of the antenna in y-z plane when the feed is $(0., \lambda, 0.)$ away from the focus.

the antenna has moved to -2.5° . The gain of the antenna in this direction is 44.37 dB. Thus, a signal incident from this direction will have a high SNR at the output of this feed while its SNR at the output of the feed at the focus will be quite low. Figures 7 and 8 show the radiation patterns of the antenna when the feed is moved two and three wavelengths, respectively, away from the focus along the positive y axis. Note that the main beam of the antenna moves further away from the z axis ($\theta = 0^\circ$) and the maximum gain of the antenna is within one dB of its value when the feed is at the focus (Figure 5). Thus, the feeds at these locations can be used very effectively to receive signals incident from angles corresponding to the sidelobes of the center-fed antenna.

Figures 9 and 10 show the radiation pattern of the antenna when the feed is moved two and three wavelengths, respectively away from the focus along the negative y axis. All other parameters are the same as in Figure 5. Note that the main beam of the antenna moves along the positive θ direction and its maximum gain is more or less unchanged. Thus, by moving the feed away from the focus along the y axis one can steer the main beam of the antenna over a wide angular region in the yz plane. Similarly, by moving the feed along the x axis, the main beam can be steered in the xz plane. Therefore, by moving the feed away from the focus of a reflector antenna, one can steer the main beam over a wide angular region without any significant loss of signal strength and

ORIGINAL PAGE IS
OF POOR QUALITY

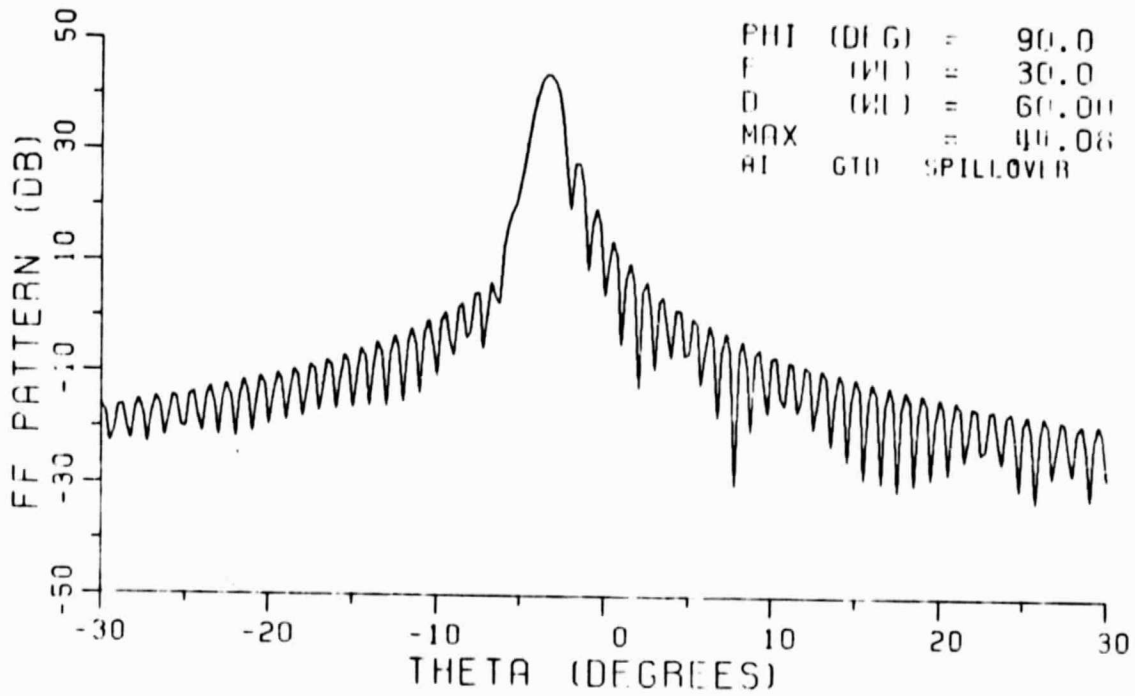


Figure 7. Radiation pattern of the antenna in y-z plane when the feed is $(i., 2\lambda, 0.)$ away from the focus.

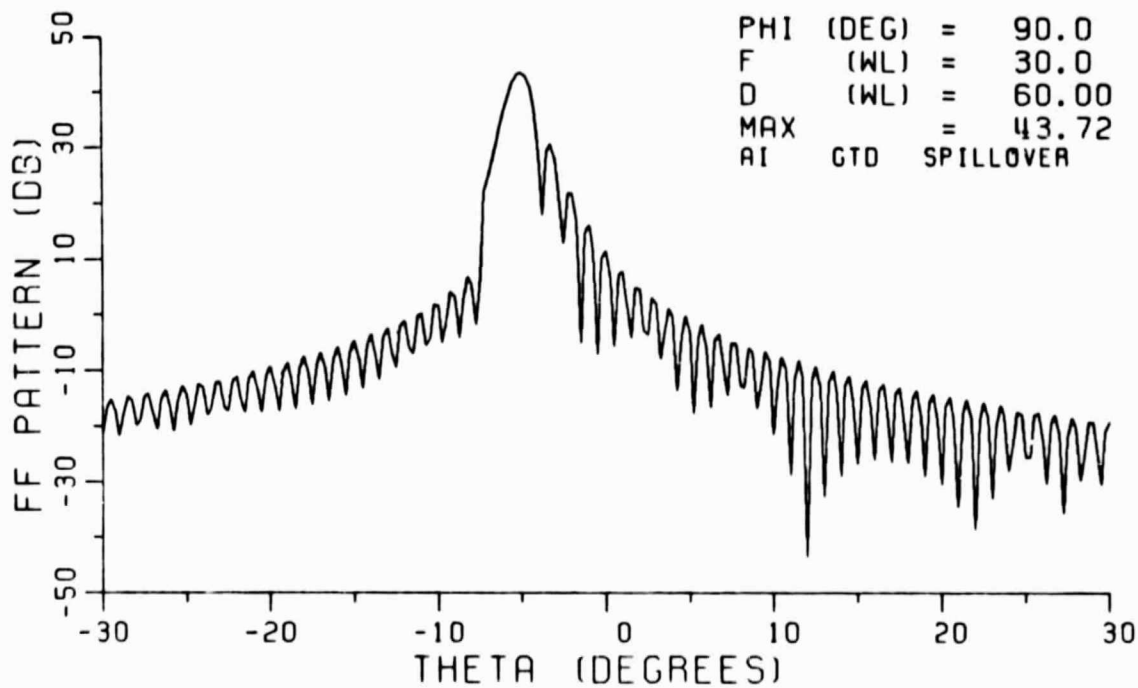


Figure 8. Radiation pattern of the antenna in y-z plane when the feed is $(0., 3\lambda, 0.)$ away from the focus.

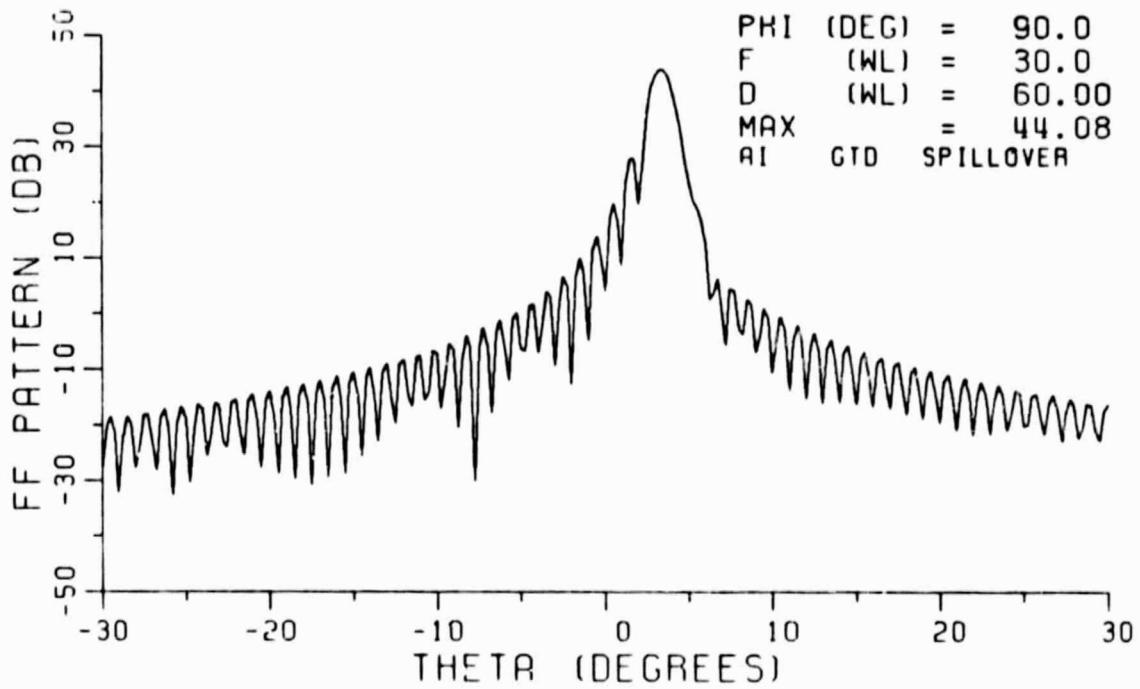


Figure 9. Radiation pattern of the antenna in y-z plane when the feed is $(0., -2\lambda, 0.)$ away from the focus.

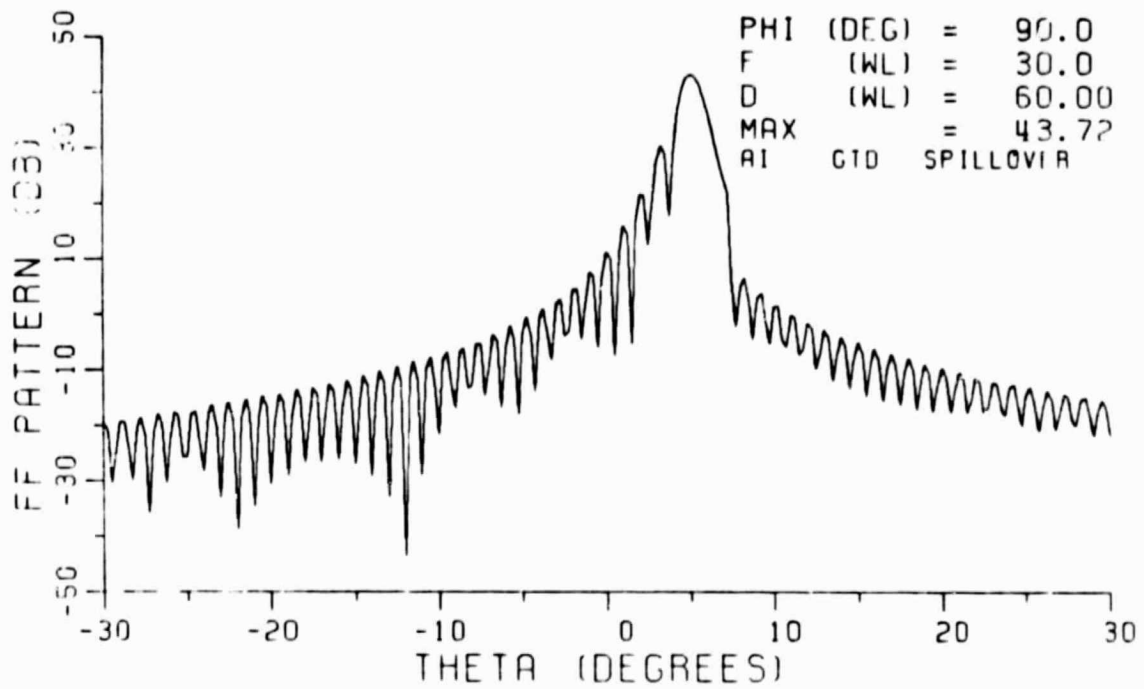


Figure 10. Radiation pattern of the antenna in y-z plane when the feed is $(0., -3\lambda, 0.)$ away from the focus.

by using an array of feeds, all signals (desired or undesired) incident on the antenna can be received with high gain, provided that the angles of arrival of the various signals are known approximately.

In our previous work [7], we have shown that by using directive auxiliary antennas in adaptive arrays, one can suppress weak interfering signals. Thus, when the main antenna is a reflector antenna, one can use defocussed feeds as auxiliary antennas to suppress weak interfering signals. The performance of such adaptive antenna arrays is studied next.

III. DEFOCUSED FEEDS AS AUXILIARY ELEMENTS

A. INTRODUCTION

In this section the performance of adaptive antenna arrays is studied when defocussed feeds of reflector antennas are used as auxiliary elements. In the communication systems under consideration, the satellites are located in geo-synchronous orbits. Thus, interfering signal sources are nearly coplanar with the desired signal source. In this work, all signals (desired and undesired) are assumed to be in the yz plane (Figure 11). The desired signal is incident along the z axis ($\theta = 0^\circ$) and to facilitate its reception one feed is located at the focus of the reflector antenna. The details of the reflector antenna were discussed in the last section. The desired signal intensity is assumed to be such that the SNR at an isotropic antenna is -30 dB. The gain of the reflector antenna in the desired signal direction is 44.51 dB (Figure 5). Thus, the SNR at the output of the feed at the focus is approximately 14.5 dB. This feed will also receive some undesired signals through the sidelobes of the reflector antenna. The interfering signals are assumed to be coherent and similar in nature to the desired signals. Adaptive arrays operating in the fully adaptive mode as well as in the sidelobe canceller mode are considered, with the fully adaptive mode discussed first.

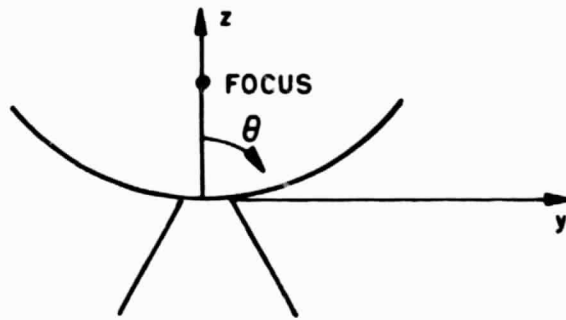
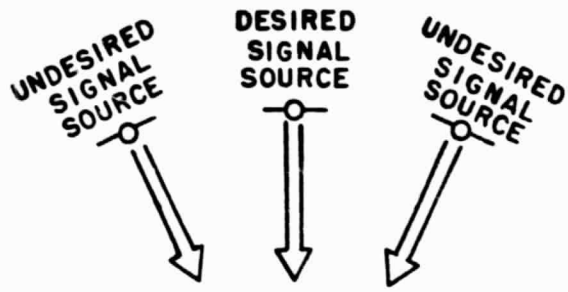


Figure 11. Source distribution in a satellite communication system.

B. FULLY ADAPTIVE ANTENNA ARRAY

Figure 12 shows the interference-to-noise ratio (INR) at the output of the feed at the focus when the signal scenario consists of a single interfering signal. The EIRP of the interfering signal is the same as that of the desired signal, i.e., the INR at an isotropic antenna is -30 dB. This case corresponds to the situation where the interference is caused by a satellite serving the same geographical area. The output INR is plotted vs. the interfering signal direction. Note that the INR is very low. In fact, the interfering signal is below the noise level by several dB (maximum output INR is -10 dB). However, this signal because of its coherent nature and its similarity to the desired signal, does cause objectionable interference and must be further suppressed.

Figure 13 shows the output INR when an additional feed (offset feed) is used and the signals received by the two feeds are weighted adaptively (Figure 14) and then summed to form the output. The offset feed is located two wavelengths away from the focus along the positive y axis. In Figure 14, G is the feedback loop gain and α defines the pole position of the low pass filter in the feedback loop. In this study, G/α is chosen to be 100. Comparing the plots in Figures 12 and 13, one can see that the interference is suppressed significantly if its angle of arrival is between -4.6° and -2.6° . The offset feed has its main beam in this angular region (Figure 7). Figure 15 shows the output SINR of the array vs. the interfering signal direction. The output SINR is

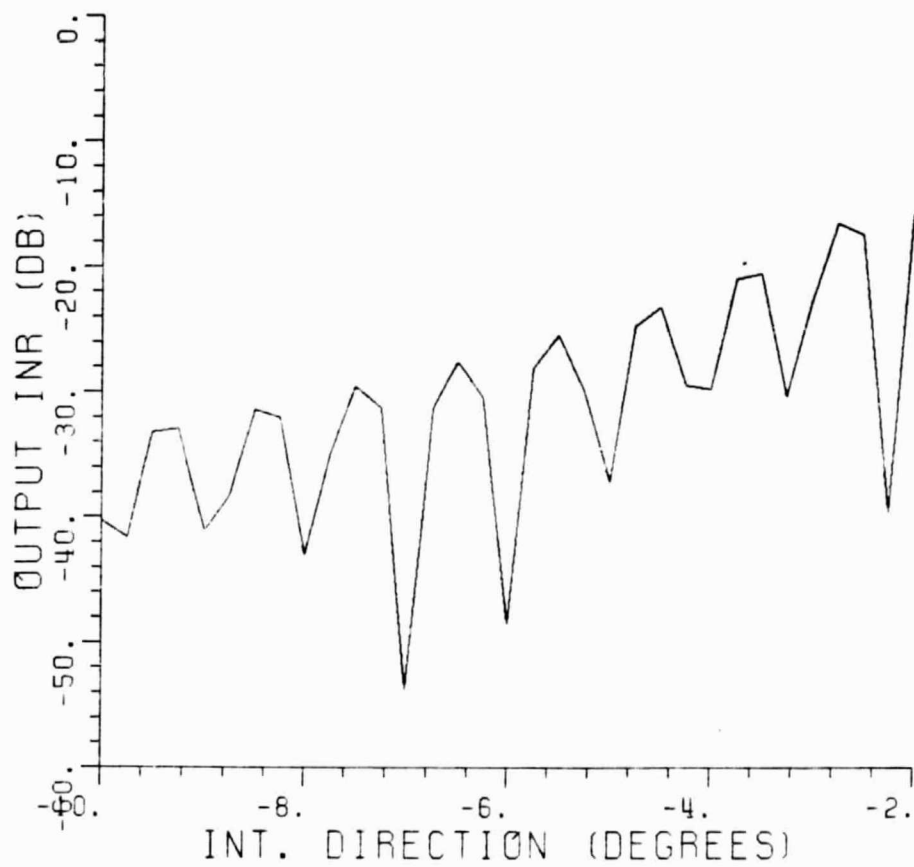


Figure 12. INR at the output of the feed at the focus vs. interfering signal direction. INR (isotropic) = -30 dB.

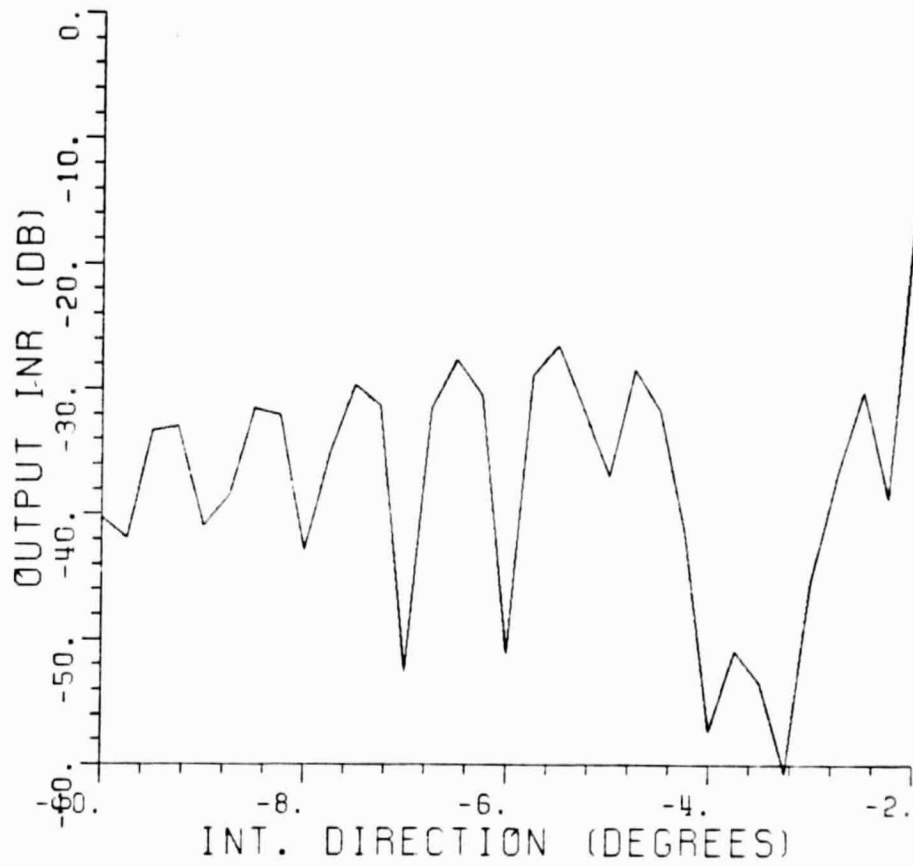
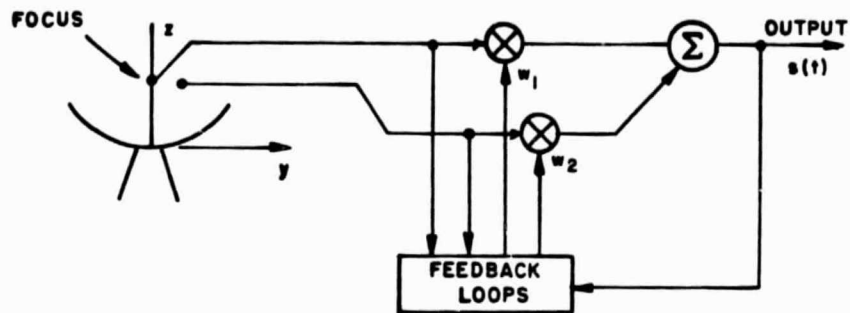
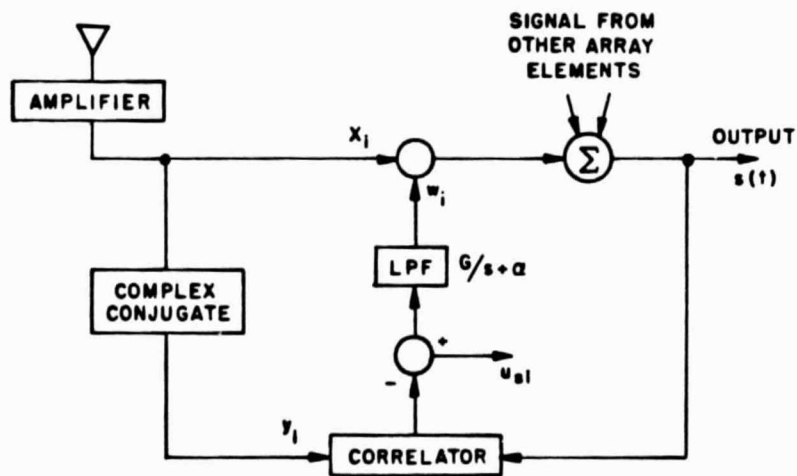


Figure 13. Output INR of a fully adaptive array vs. interfering signal direction. One offset feed at $(0., 2\lambda, 0.)$, $G/\alpha = 100$. INR (isotropic) = -30 dB.



(a)



(b)

Figure 14. Fully adaptive array with one offset feed (a) and a typical feedback loop (b).

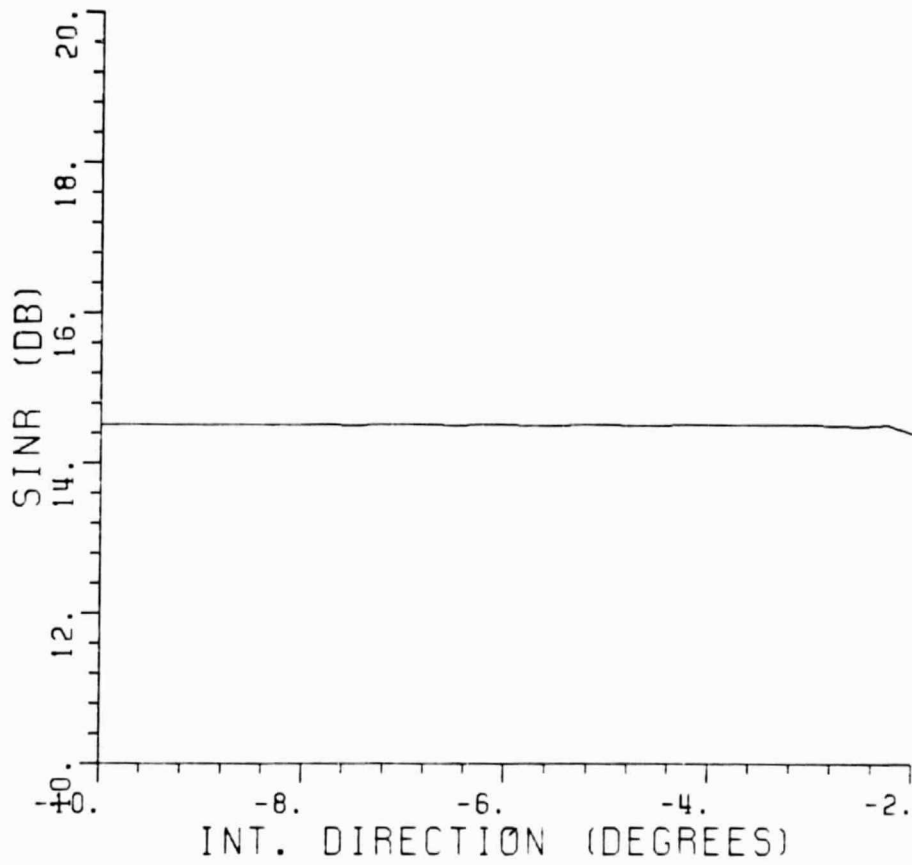


Figure 15. Output SINR of a fully adaptive array vs. interfering signal direction. One offset feed at $(0., 2\lambda, 0.)$, INR (isotropic) = -30 dB, $G/\alpha = 100$.

approximately 14.5 dB for all angles of arrival of the interfering signal. Thus, the interference is suppressed without adversely affecting the desired signal or SNR. Hence offset feeds of a reflector antenna can be used as auxiliary elements of an adaptive array to suppress a weak interfering signal provided the interfering direction is approximately known and the offset feeds are so located as to steer the main beam of the reflector antenna in that general direction.

Figures 16 and 17 show the output INR and output SINR of the adaptive array when the offset feed is moved three wavelengths away from the focus along the positive y axis. All other parameters are the same as in Figures 13 and 15, respectively. Now the main beam of the reflector using the offset feeds is along -5.5° (Figure 8) and one can see that if the interference is incident from this angular region, it is suppressed by the adaptive array without affecting the output SINR.

From the above discussion, it is clear that when offset feeds of a reflector antenna are used as auxiliary elements of an adaptive array to cancel weak interfering signals, the approximate angular locations of the sources of interference should be known. This constraint can be removed by using an array of offset feeds. These offset feeds should be distributed such that the whole angular region of expected interference is covered. Figure 18 shows the output INR of the adaptive array when two offset feeds are used as two auxiliary elements of the adaptive array. The two offset feeds are located two and three wavelengths,

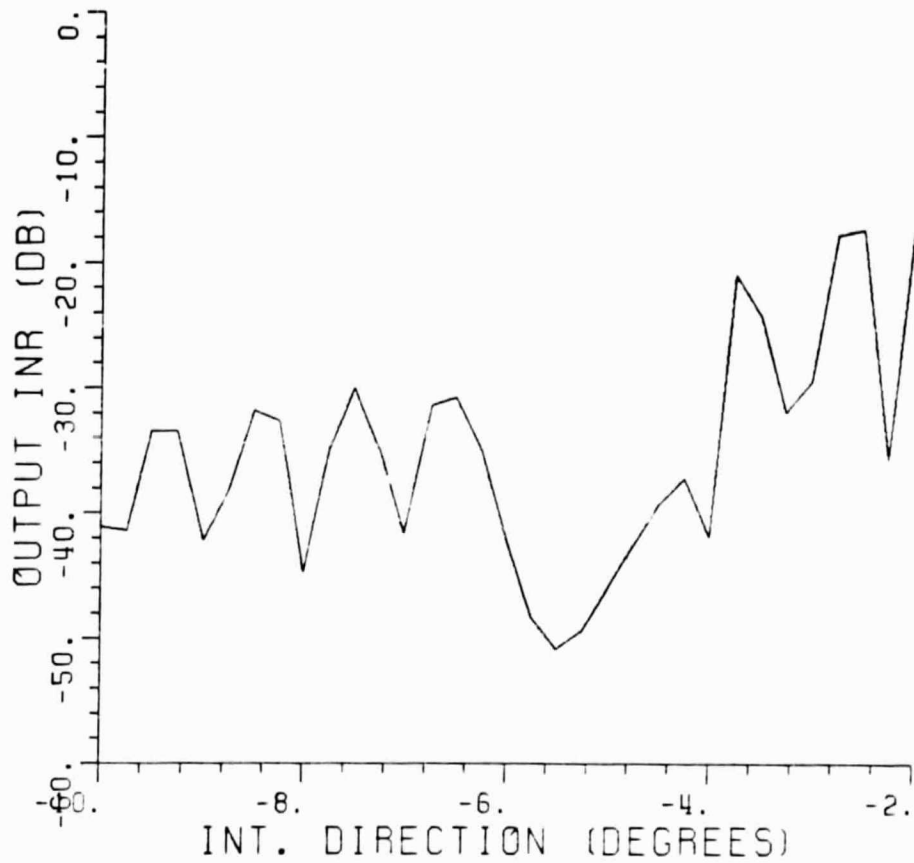


Figure 16. Output INR of a fully adaptive array vs. interfering signal direction. One offset feed at $(0., 3\lambda, 0.)$, INR (isotropic) = -30 dB, $G/\alpha = 100$.

ORIGINAL PAGE IS
OF POOR QUALITY

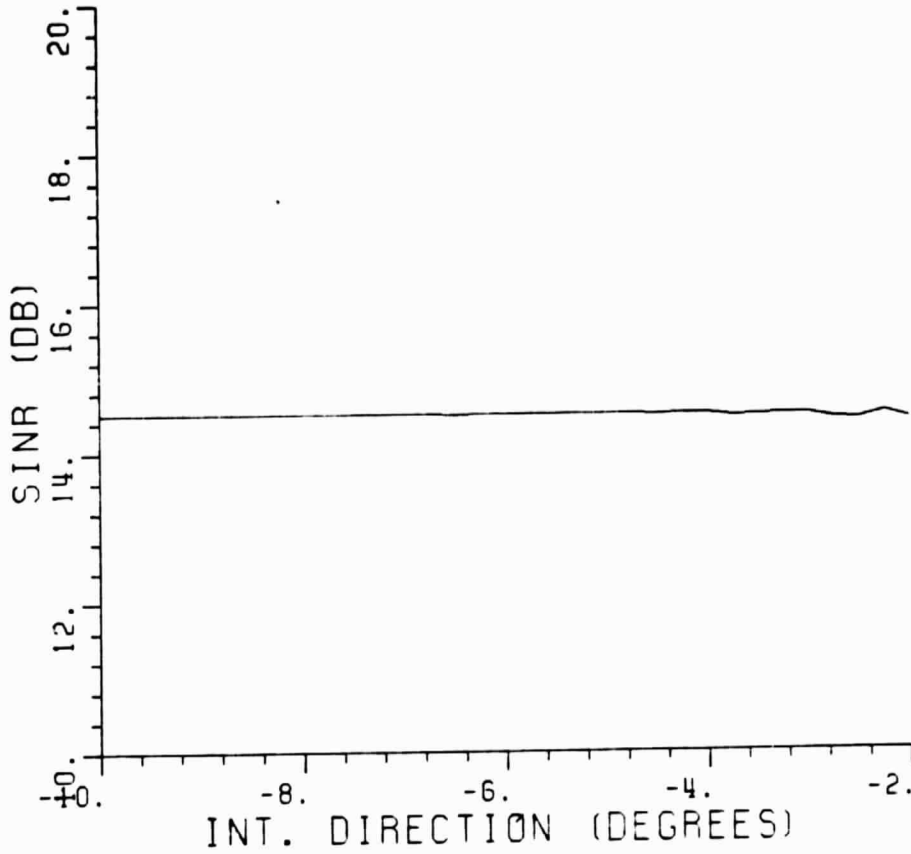


Figure 17. Output SINR of a fully adaptive array vs. interfering signal direction. One offset feed at $(0., 3\lambda, 0.)$, INR (isotropic) = -30 dB, $G/\alpha = 100$.

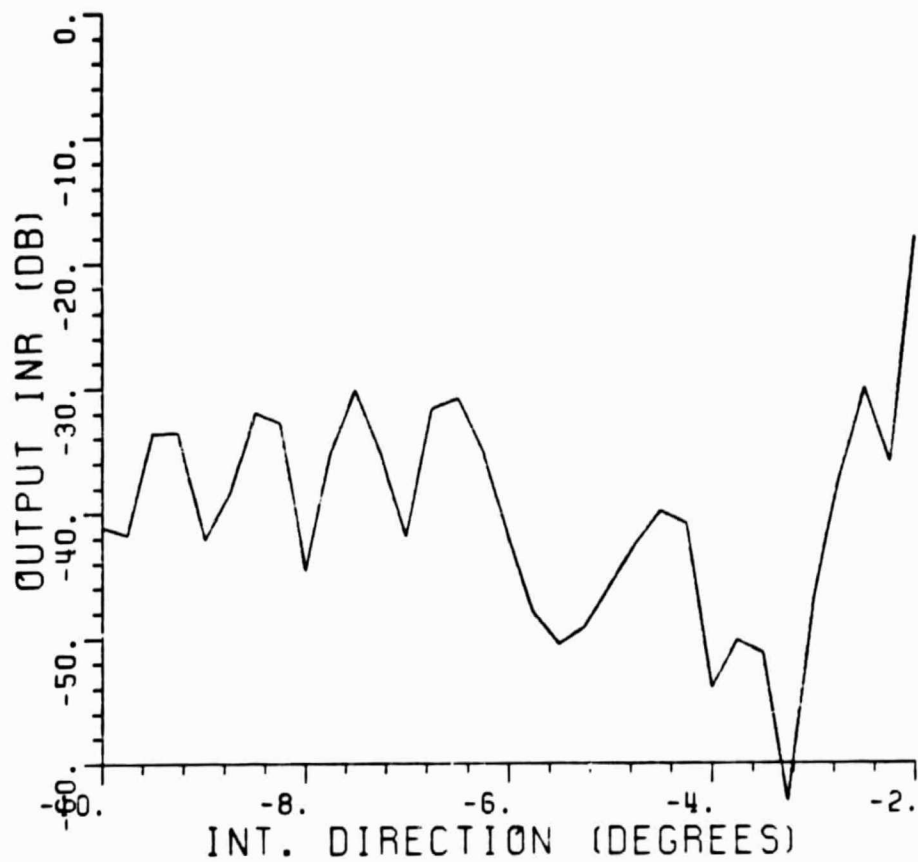


Figure 18. Output INR of a fully adaptive array vs. interfering signal direction. Two offset feeds at $(0., 2\lambda, 0.)$ and $(0., 3\lambda, 0.)$, respectively. INR (isotropic) = -30 dB, $G/\alpha = 100$.

respectively, away from the focus along the positive y axis. All other parameters are the same as in Figure 13. Comparing the plots in Figures 12 and 18, one can see that interference is suppressed significantly if its angle of arrival is between -6.5° and -2.6° . Thus, the angular region in which the interference can be suppressed has increased significantly over the one offset feed case (Figure 13 or Figure 16).

In the above discussion, the EIRP of the desired signal and the interfering signal were assumed to be the same. This situation corresponds to the case of multiple satellites serving the same geographical area. The interference can also be caused by satellites serving different areas. In such situations, the EIRP of the interfering signals will be 10-20 dB below that of the desired signal. These interfering signals enter the receiver through the antenna sidelobes. Thus, the signal-to-interference ratio in the receiver will be 40-50 dB and INR in the receiver will be -25 to -35 dB (SNR is -15 dB). These interfering signals, in practice, will not cause any objectionable interference. However, for the sake of completeness are discussed next.

Figure 19 shows the INR at the output of the feed located at the focus of the reflector antenna vs. the interfering signal direction. The EIRP of the interfering signal is 10 dB below that of the desired signal, i.e., the INR at an isotropic antenna is -40 dB. Note that the INR is very low. Figure 20 shows the output INR when an additional feed is used and the signal received by two feeds are adaptively weighted and

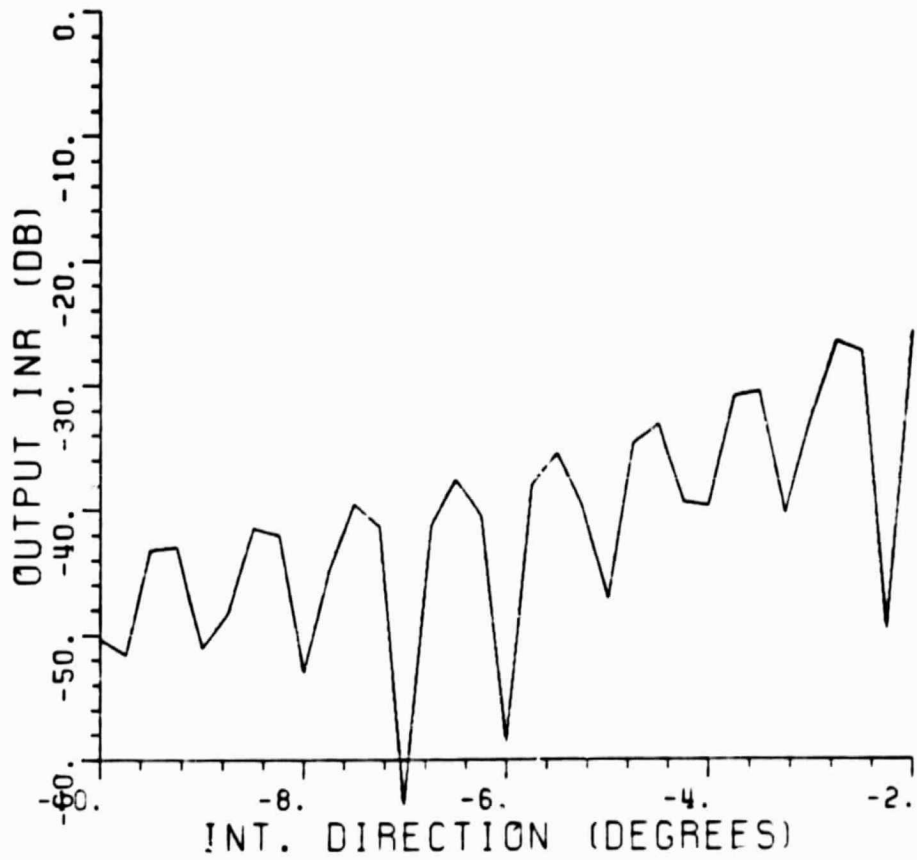


Figure 19. INR at the output of the feed at the focus vs. interfering signal direction. INR (isotropic) = -40 dB.

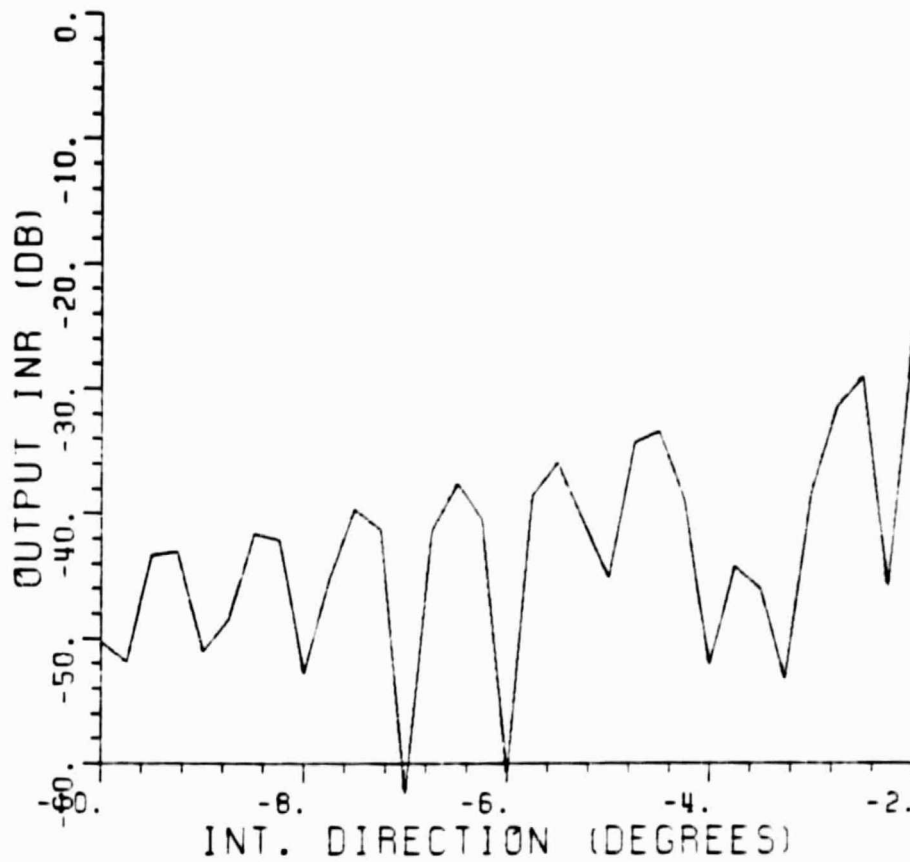


Figure 20. Output INR of a fully adaptive array vs. the interfering signal direction. One offset feed at $(0., 2\lambda, 0.)$, INR (isotropic) = -40 dB, $G/\alpha = 100$.

then summed to form the output. The additional feed is located two wavelengths away from the focus of the reflector along the positive y axis. Comparing the plots in Figures 19 and 20, one can see that the maximum interference suppression is approximately 12 dB, which may not be sufficient for certain applications. Figure 21 shows the output INR when two offset feeds are used as two auxiliary elements of the adaptive array. The two offset feeds are located two and three wavelengths, respectively, away from the focus along the positive y axis. All other parameters are the same as in Figure 20. Comparing the plots in Figures 19, 20 and 21, one can see that the angular region in which the interference is suppressed has increased over the one offset feed case. The increase in the angular region is, however, very small. Further, the maximum interference suppression is still only 12 dB. Other methods of interference suppression, therefore, should be combined with the above technique if further interference suppression is needed.

In our previous work [6,7] under this grant, we have shown that by using modified feedback loops, one can significantly increase the interference suppression. In the modified feedback loops, the noise level in the feedback loop is reduced by reducing the correlation between the noise components of the two inputs to the correlator in the feedback loops. The higher the noise decorrelation, the stronger the interference suppression. However, before studying the performance of the adaptive array with modified loops, its performance in the sidelobe

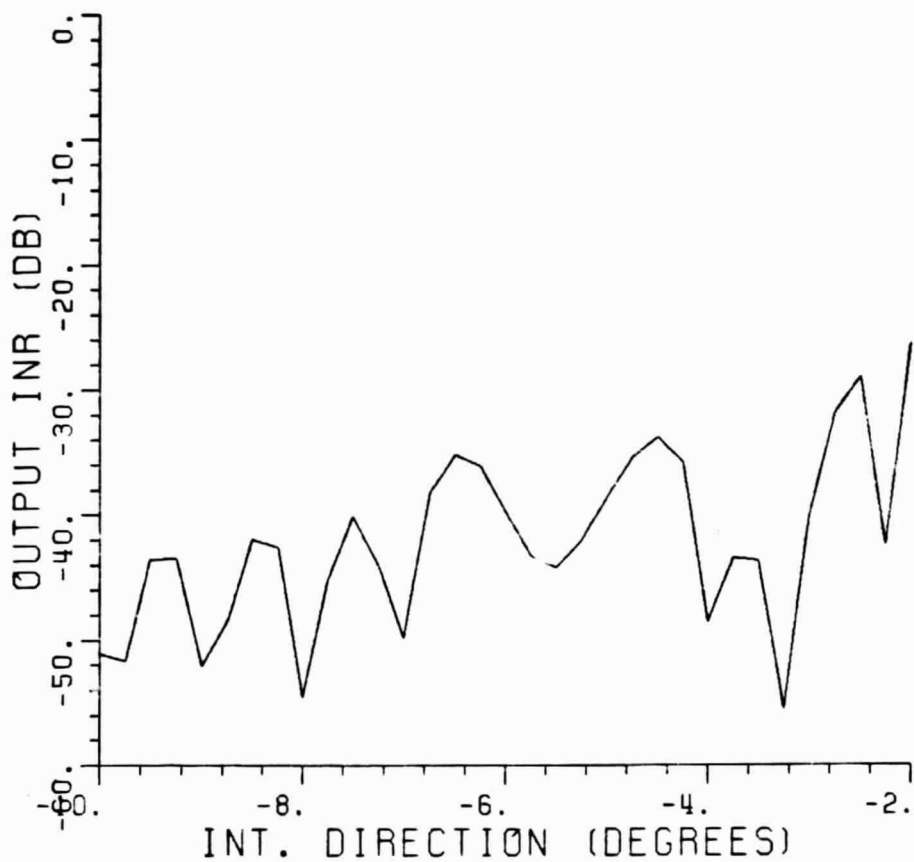


Figure 21. Output INR of a fully adaptive array vs. the interfering signal direction. Two offset feeds at $(0., 2\lambda, 0.)$ and $(0., 3\lambda, 0.)$, respectively. INR (isotropic) = -30 dB, $G/\alpha = 100$.

canceller mode is studied. It is shown that the performance in the two modes (fully adaptive and sidelobe canceller) is approximately the same. Thus, either adaptive mode can be used to suppress the interfering signals.

C. THE PERFORMANCE OF A SIDELOBE CANCELLER

In the above discussion, the adaptive array was operated in a fully adaptive mode, i.e., the output of the feed at the focus as well as the outputs of the offset feeds were adaptively weighted. In this subsection, the performance of a sidelobe canceller is studied. In the sidelobe canceller, the output of the main antenna (feed at the focus in the present case) has a fixed weight while the outputs of the auxiliary antennas (offset feeds) are adaptively weighted (Figure 22). Thus the total number of feedback loops is one less than in the fully adaptive mode. However, as pointed out in our earlier work [7], one should know the desired signal strength fairly accurately to avoid SNR degradation.

Figures 23 and 24 show the output INR of the array when a single offset feed is located at two and three wavelengths, respectively, away from the focus of the antenna along the positive y axis. The array is operated in the sidelobe canceller mode. The EIRP of the interfering signal is assumed to be such that the INR at an isotropic antenna is -30 dB. Comparing the output INR of the sidelobe canceller with that of the fully adaptive array (Figures 13 and 16, respectively) one can see that the interference suppression in the two modes is approximately the

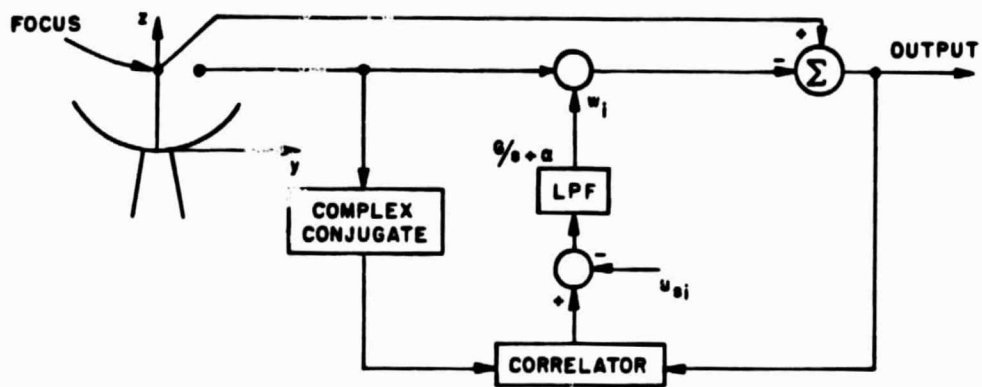


Figure 22. Sidelobe canceller with one offset feed.

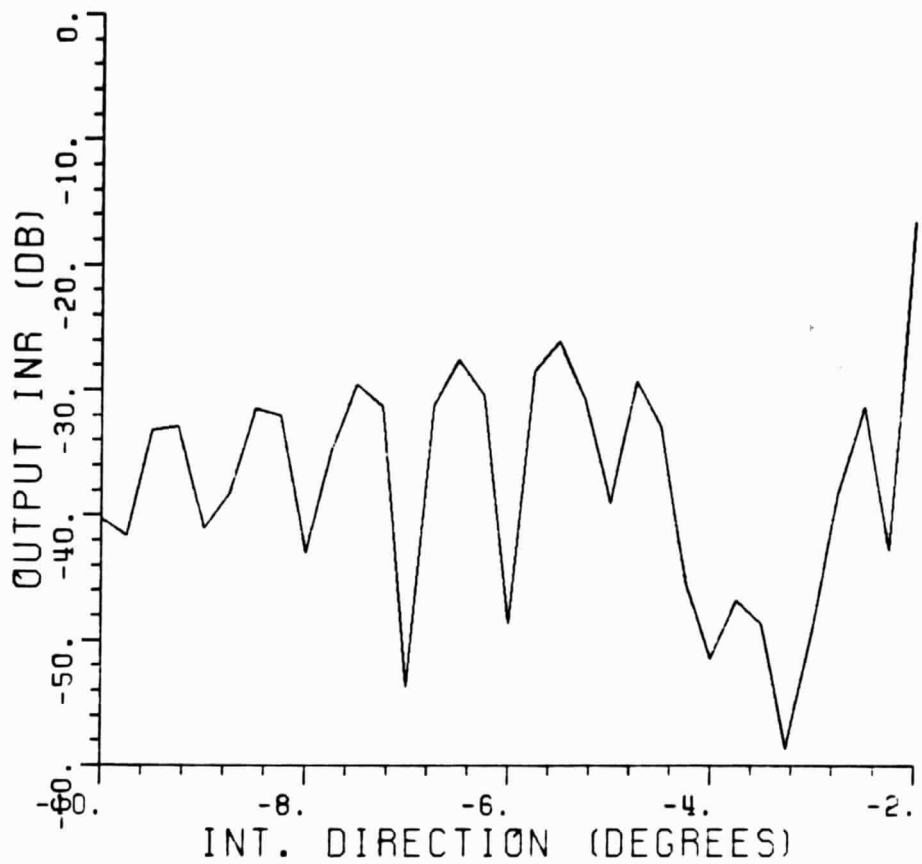


Figure 23. Output INR of a sidelobe canceller vs. the interfering signal direction. One offset feed at $(0., 2\lambda, 0.)$, INR (isotropic) = -30 dB, $G/\alpha = 100$.

ORIGINAL PAGE IS
OF POOR QUALITY

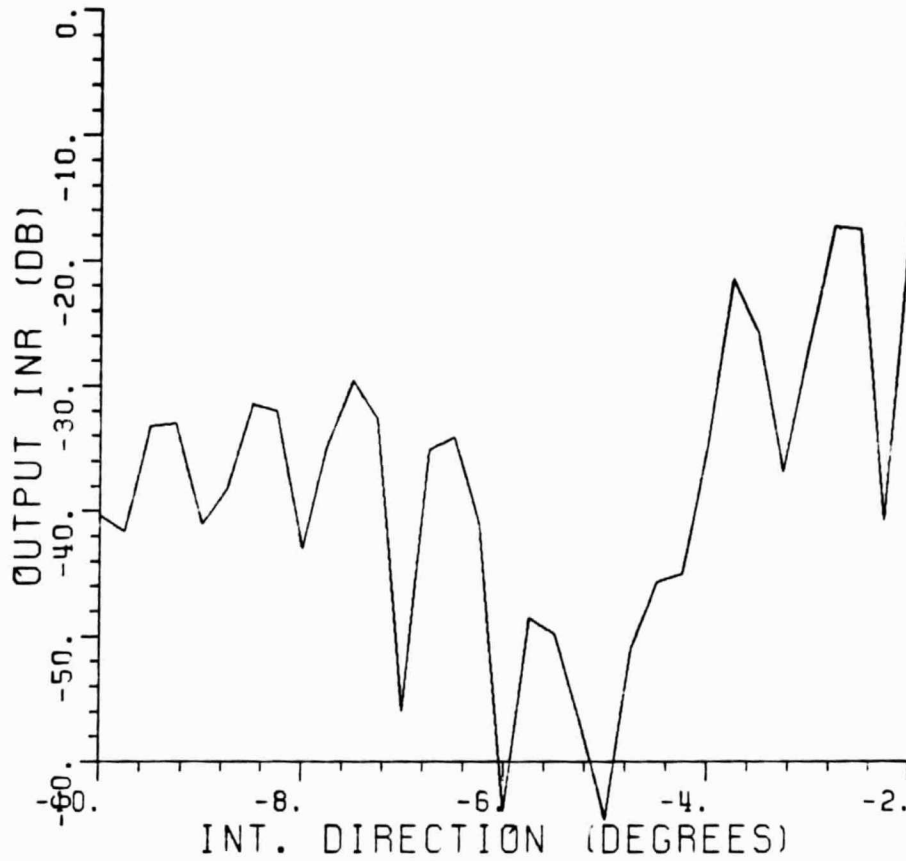


Figure 24. Output INR of a sidelobe canceller vs. the interfering signal direction. One offset feed at $(0., 3\lambda, 0.)$, INR (isotropic) = -30 dB, $G/\alpha = 100$.

same. Thus, either arrangement, sidelobe canceller or fully adaptive array, can be used to suppress the interfering signal. Figures 25 and 26 show the output SINR of the sidelobe canceller for the two locations of the offset feed. The output SINR in both cases is approximately 14.5 dB which is equal to the SNR in the feed at the focus. Thus, the interference is suppressed without adversely affecting the desired signal or SNR.

Figure 27 show the output INR when two offset feeds located at two and three wavelengths, respectively, away from the focus along the positive y axis are used as two auxiliary elements. All other parameters are the same as above. Comparing the INR plot in Figure 27 with those in Figures 23 and 24, one can see that the angular region in which the interference has been suppressed has increased. Thus, by using an array of offset feeds, one can take care of uncertainty in the location of the interfering signal sources. Again, the interference suppression obtained using the sidelobe canceller is approximately equal to the interference suppression provided by a fully adaptive array (Figure 18).

Figure 28 shows the output INR of the array when the EIRP of the interfering signal is such that the INR at an isotropic antenna is -40 dB. All other parameters are the same as in Figure 27. Comparing the out INR in Figure 28 with that of the output INR of the fully adaptive array (Figure 21) one can see the angular region in which the interference is suppressed is a little larger in the case of the

ORIGINAL PAGE IS
OF POOR QUALITY

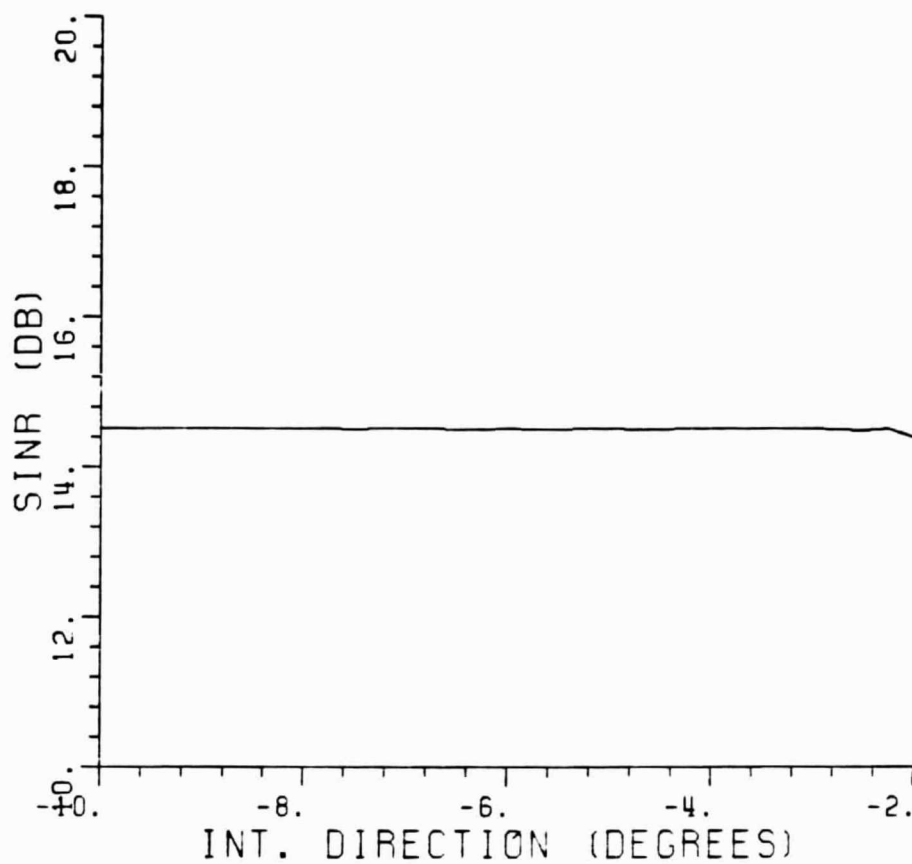


Figure 25. Output SINR of a sidelobe canceller vs. the interfering signal direction. One offset feed at $(0., 2\lambda, 0.)$, INR (isotropic) = -30 dB, $G/\alpha = 100$.

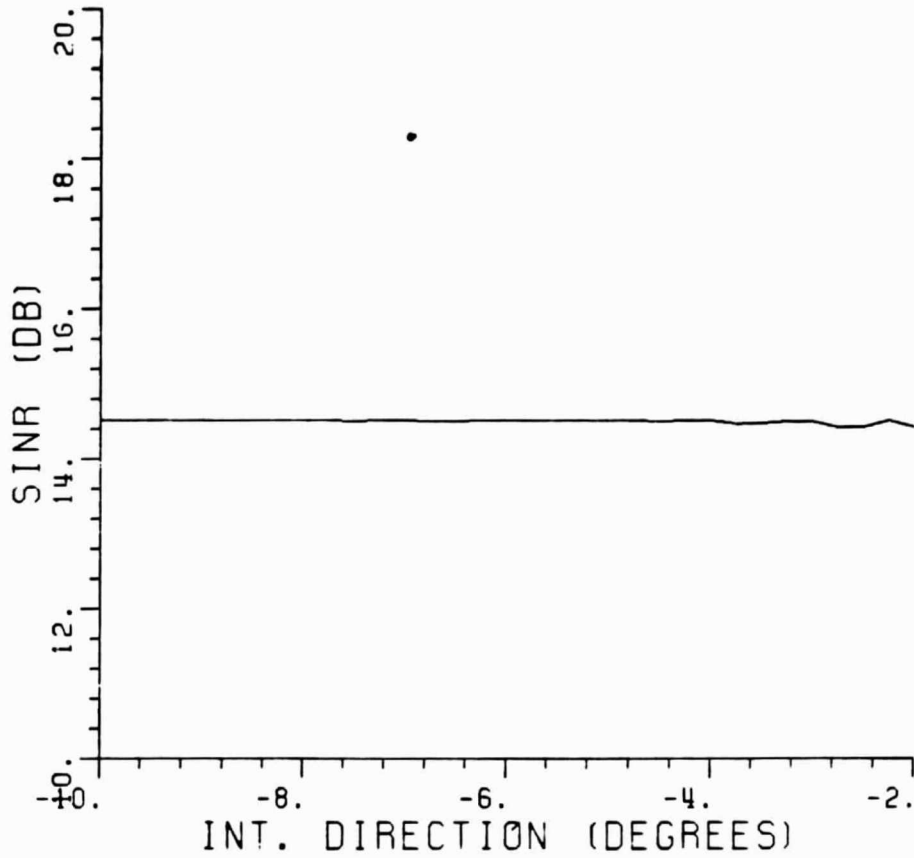


Figure 26. Output SINR of a sidelobe canceller vs. the interfering signal direction. One offset feed at $(0., 3\lambda, 0.)$, INR (isotropic) = -30 dB, $G/\alpha = 100$.

ORIGINAL PAGE IS
OF POOR QUALITY

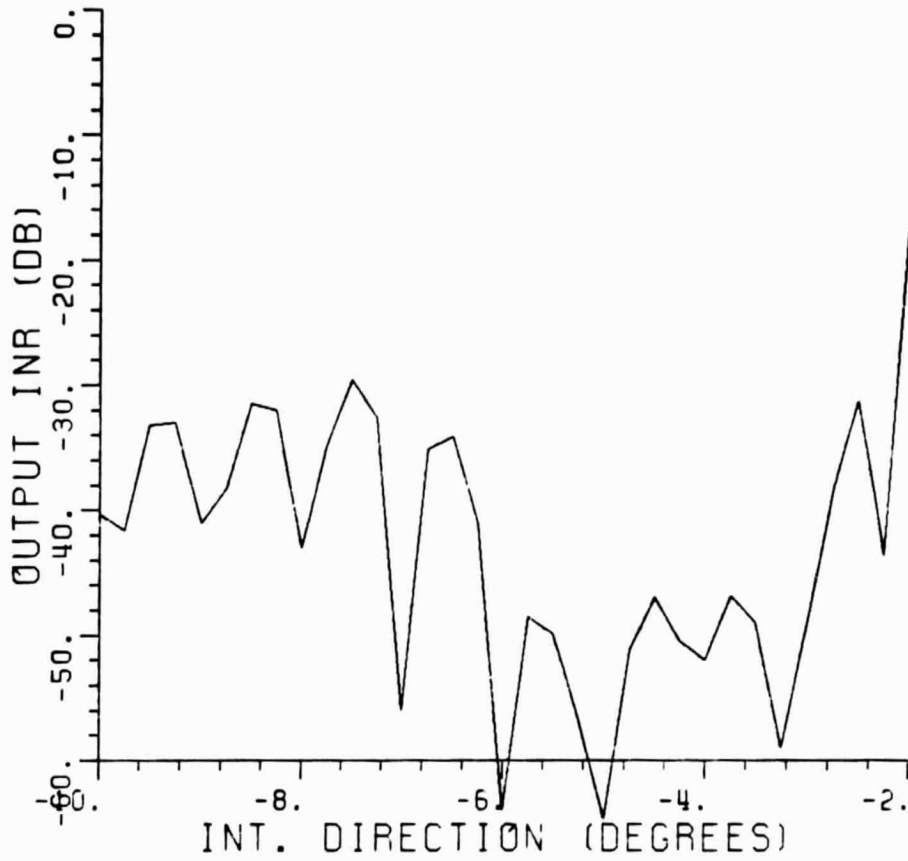


Figure 27. Output INR of a sidelobe canceller vs. the interfering signal direction. Two offset feeds at $(0., 2\lambda, 0.)$ and $(0., 3\lambda, 0.)$, respectively. INR (isotropic) = -30 dB, $G/\alpha = 100$.

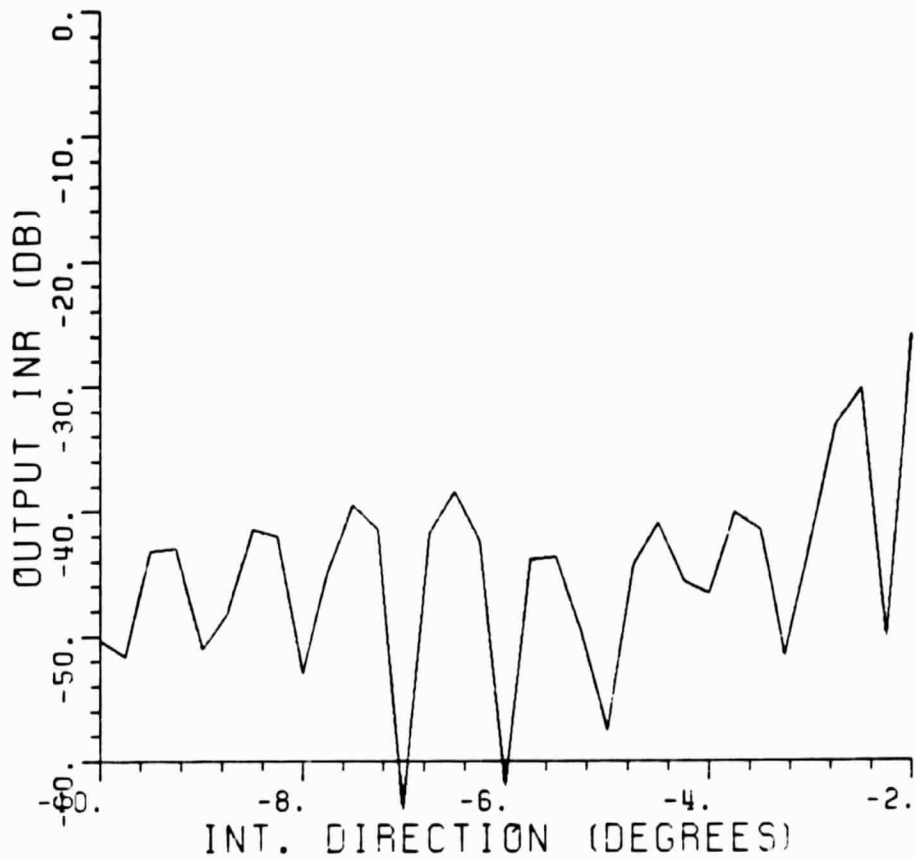


Figure 28. Output INR of a sidelobe canceller vs. the interfering signal direction. Two offset feeds at $(0., 2\lambda, 0.)$ and $(0., 3\lambda, 0.)$, respectively. INR (isotropic) = -40 dB, $G/\alpha = 100$.

sidelobe canceller. The maximum interference suppression by the two adaptive arrays is, however, the same. Thus, either adaptive array can be used for interference suppression. Therefore, from here on, only the sidelobe canceller mode will be considered.

Comparing the output INR in Figure 28 with that of output INR at the feed at the focus (Figure 19), we see that the maximum interference suppression is only 12 dB, which may not be sufficient for some applications. Other methods of interference suppression, therefore, should be combined with the above technique. As pointed out before, one can use modified feedback loops to enhance the interference suppression. The performance of the sidelobe canceller with modified feedback loops is studied next.

D. SIDELOBE CANCELLER WITH MODIFIED FEEDBACK LOOPS

In our previous work [6,7], we reported on the suppression of weak interfering signals by means of modified feedback loops. The performance of various adaptive arrays was studied when modified feedback loops were used to control the array weights. In the modified feedback loops, the noise level in the feedback loops is reduced by reducing the correlation (ρ) between the noise components of the two inputs to the correlator in the feedback loops. For conventional feedback loops, the noise correlation, ρ , is equal to

unity[†]. It was shown that the higher the noise decorrelation ($\rho \rightarrow 0$), the stronger the interference suppression. In this subsection, the interference suppression provided by the sidelobe canceller (discussed above) is studied when modified feedback loops are used to control the weights of the auxiliary elements (output of offset feeds).

Figure 29 shows the output INR of the sidelobe canceller with one auxiliary element. The auxiliary element is an offset feed located two wavelengths away from the focus of the reflector antenna. A modified feedback loop is used to control the weight of the auxiliary antenna. The INR at an isotropic antenna is -30 dB. The output INR is plotted vs. the interfering signal direction for various values of ρ , the noise correlation in the feedback loops. As expected, the interference suppression increases with an increase in noise decorrelation. The angular region in which the interference is suppressed also increases with an increase in the noise correlation. The reason for this is that by reducing the noise in the feedback loops, the threshold above which the signals are suppressed is lowered. Thus, one does not need very high gain auxiliary antennas to suppress weak interfering signals, and the interference signals outside the HPBW of the auxiliary antennas are also suppressed. Therefore, more uncertainty in the location of the interfering signal sources can be tolerated.

[†]The noise correlation, ρ , in this work is defined as the correlation between the thermal noise in the signal branch of the feedback loop with the thermal noise in the correlation branch of the feedback loop (see Figures 13 and 22).

ORIGINAL PAGE IS
OF POOR QUALITY

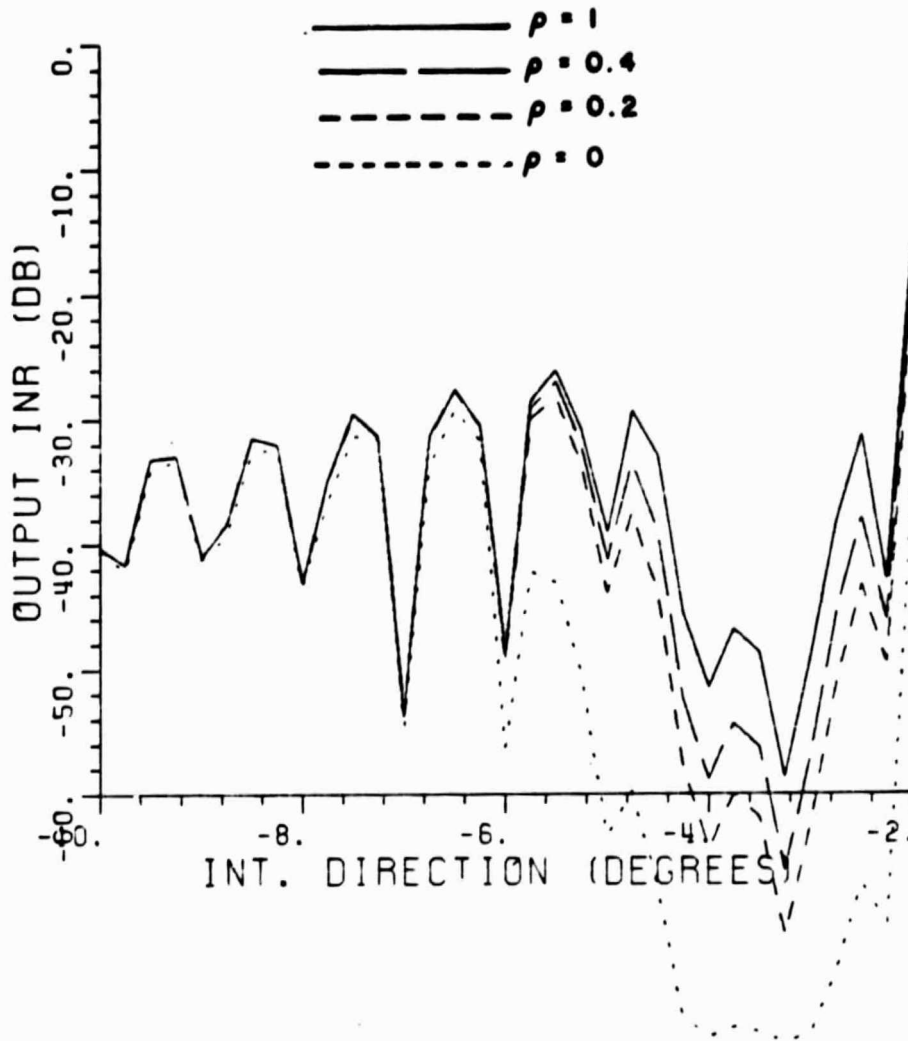


Figure 29. Output INR of a sidelobe canceller vs. the interfering signal direction. One offset feed at $(0., 2\lambda, 0.)$ and modified feedback loop is used. INR (isotropic) = -30 dB, $G/\alpha = 100$.

Figure 30 shows the output INR of the sidelobe canceller when the INR at an isotropic antenna is -40 dB. All other parameters are the same as in Figure 29. Again, the interference suppression increases with an increase in noise decorrelation. The angular region in which the interference is suppressed also increases with an increase in noise decorrelation. Thus, offset feeds of a reflector antenna in conjunction with modified feedback loops can be used very effectively to suppress weak interfering signals.

As pointed out before, in the modified feedback loops, the noise level in the feedback loops is reduced by reducing the correlation between the noise components of the two inputs to the correlator in the feedback loop. Two techniques to reduce the noise correlation were presented in our previous work [6]. When the internal thermal noise is the main noise source, two different amplifiers (Figure 31) can be used to reduce noise correlation. In this case, the output INR will be given by the family of curves given in Figure 29 and 30. Depending upon the noise correlation achieved one can find the interference suppression.

When the dominant noise source is external, two separate antennas each followed by its own amplifier (Figure 32) should be employed to provide noise decorrelation. The noise entering the two antennas should be uncorrelated while the signals from the interfering source should arrive at both antennas with the same phase. Thus this scheme requires twice the number of auxiliary antennas and a careful distribution of

ORIGINAL PAGE IS
OF POOR QUALITY

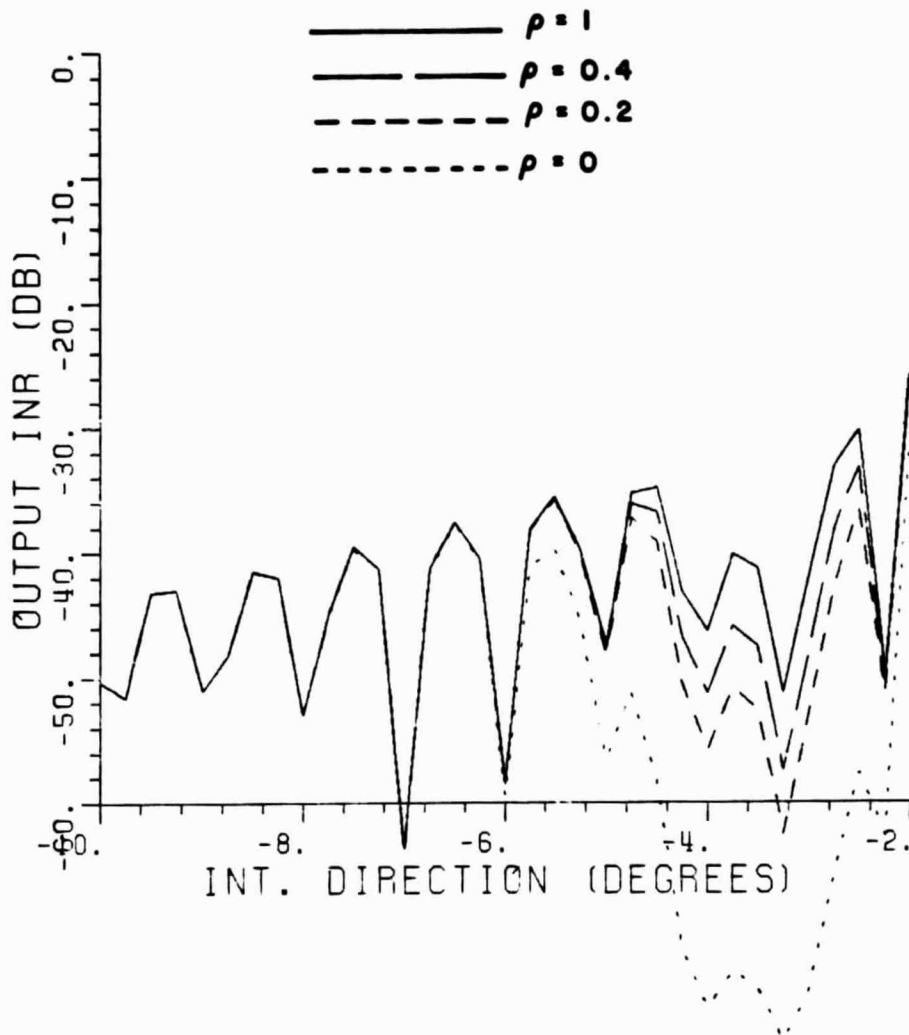


Figure 30. Output INR of a sidelobe canceller vs. the interfering signal direction. INR (isotropic) = -40 dB. Other parameters are the same as in Figure 29.

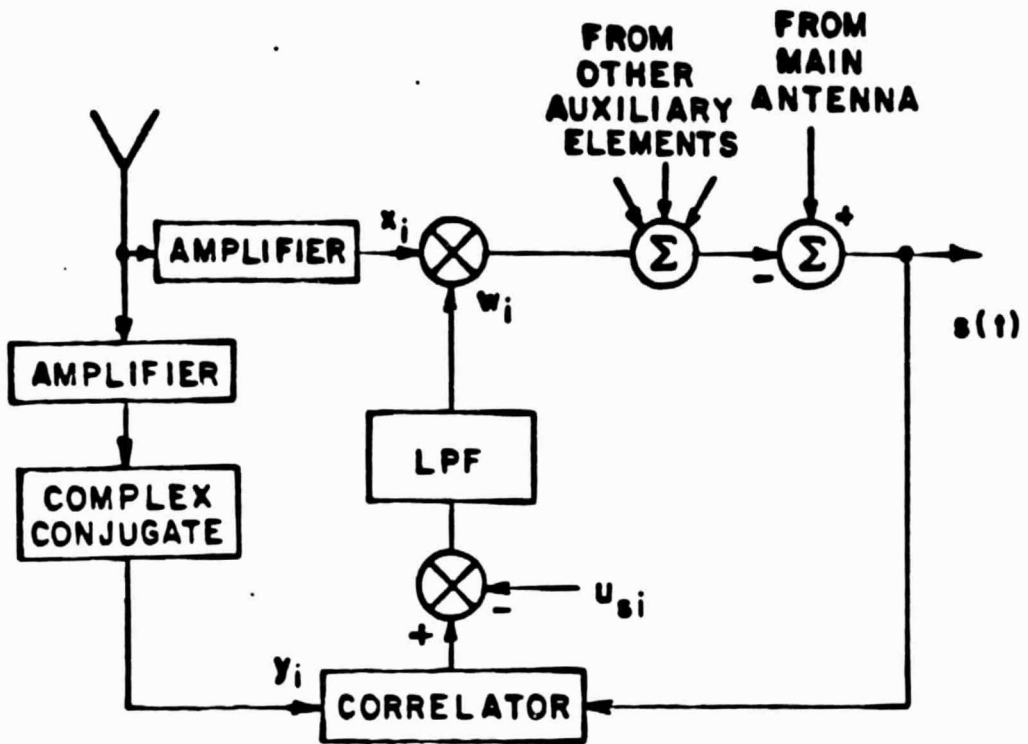


Figure 31. Feedback loop with two amplifiers.

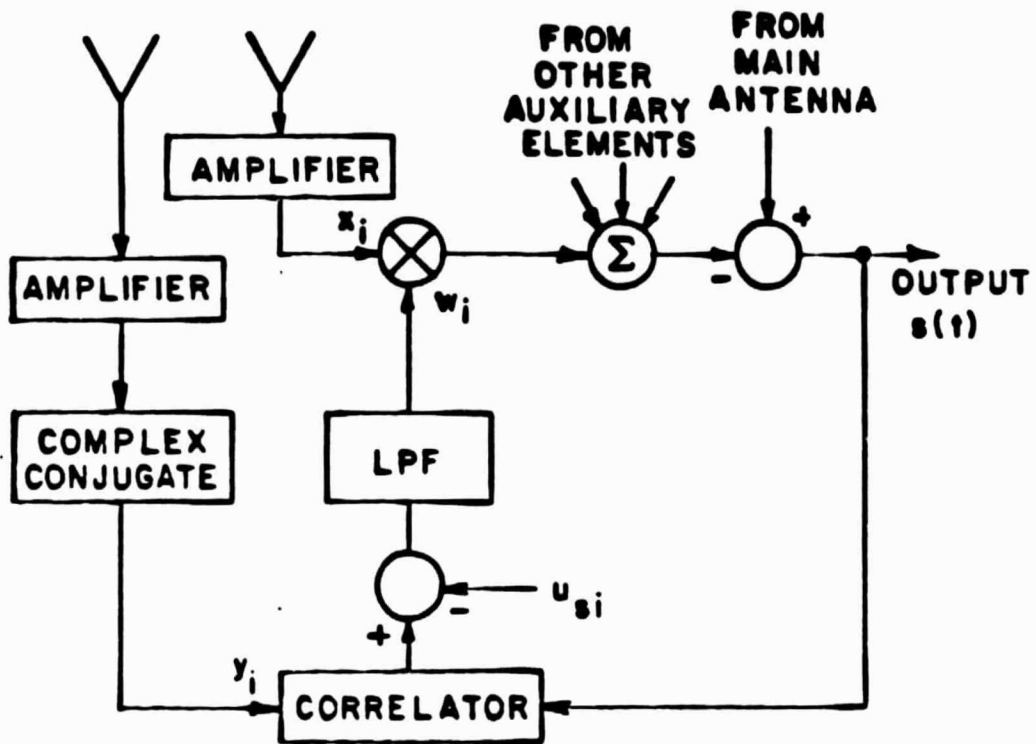


Figure 32. Feedback loop with two antennas.

auxiliary antennas. However, it provides more noise decorrelation than a feedback with two amplifiers and applies to both external and internal noise. Next, we will show that offset feeds of a reflector antenna can be used to meet the above requirements.

E. NOISE DECORRELATION USING OFFSET FEEDS

In appendix A, the correlation between the noise entering two antennas displaced from each other is evaluated. It is shown that if the external noise is uniformly distributed across the visible range, complete noise decorrelation may be obtained from two isotropic antennas spaced half a wavelength apart. At any separation larger than half a wavelength, the noise correlation is relatively small and decreases as the separation increases. Further, it is shown that the noise correlation decreases as the system bandwidth increases. In the case of directive antennas, it is shown that the two antennas may be pointed in different directions to decorrelate the noise. In this case, the noise entering the two antennas arrives from mostly different portions of the observation range and thus assures relatively small noise correlation. The noise correlation further decreases with spatial separation between the two antennas.

In the case of a reflector antenna, as shown before, one can steer the main beam in various directions by moving the feed away from the focus. Thus, noise entering the various feeds located at different

locations will be relatively independent. Therefore, one can use two separate offset feeds each followed by its own amplifier for each feedback loop to provide noise decorrelation. In the present application, however, it is important that the signal from the interfering source arrive at the two feeds with the same phase. This requirement, as explained below, can be met, though with some reduction in the antenna gain in the interfering signal direction.

In the communication systems under consideration, the satellites are located in geo-synchronous orbits. Thus the interfering signal sources are nearly coplanar with the desired signal source. Therefore, if two antennas are placed symmetrically along a line orthogonal to this plane, the signals received by the two antennas will be in phase. In our study, we have assumed all signals to be in the yz plane. Thus, signals received by two antennas located at (x_i, y_i, z_i) and $(-x_i, y_i, z_i)$ will have the same phase, where x_i, y_i, z_i are arbitrary. In the case of a reflector antenna, the two feeds will be located at the same y and z coordinates but equal and opposite x coordinates.

Figure 33 shows the phase of the field radiated by the reflector antenna when the feed is located at $(0.5\lambda, 2\lambda, 0.)$ with respect to the focus of the antenna. The phase is measured in the yz plane ($\phi = 90^\circ$) and is plotted vs. θ . Figure 34 shows the phase of the radiated field when the feed is moved to $(-0.5\lambda, 2\lambda, 0.)$. Note that the phase of the radiated field for the two locations of the feed is exactly the same.

ORIGINAL PAGE IS
OF POOR QUALITY

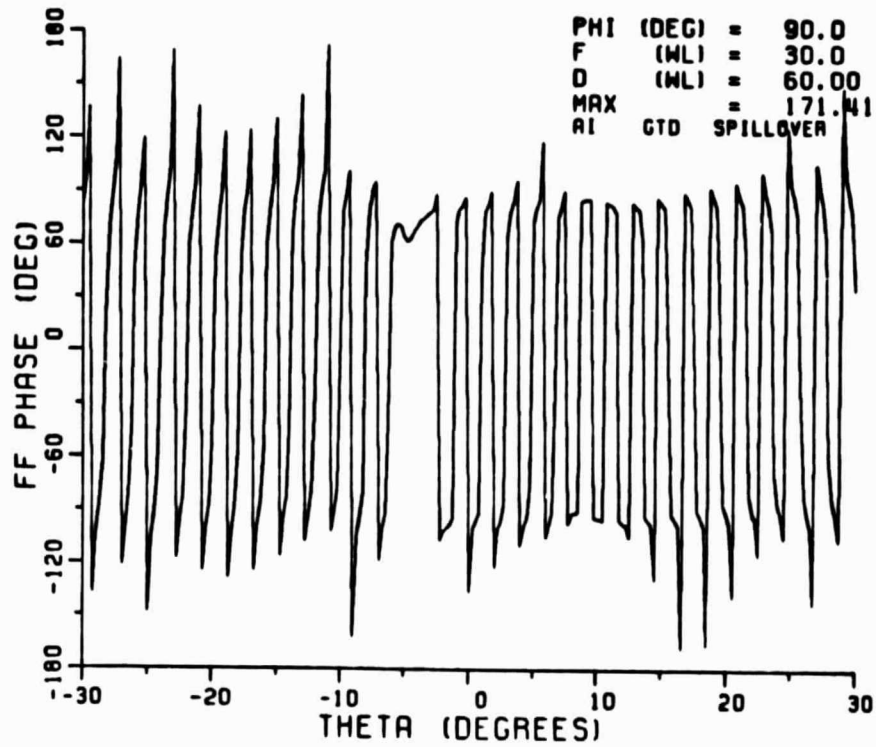


Figure 33. Phase of the radiated field in the yz plane when the feed is $(0.5\lambda, 2\lambda, 0.)$ away from the focus.

ORIGINAL PAGE IS
OF POOR QUALITY

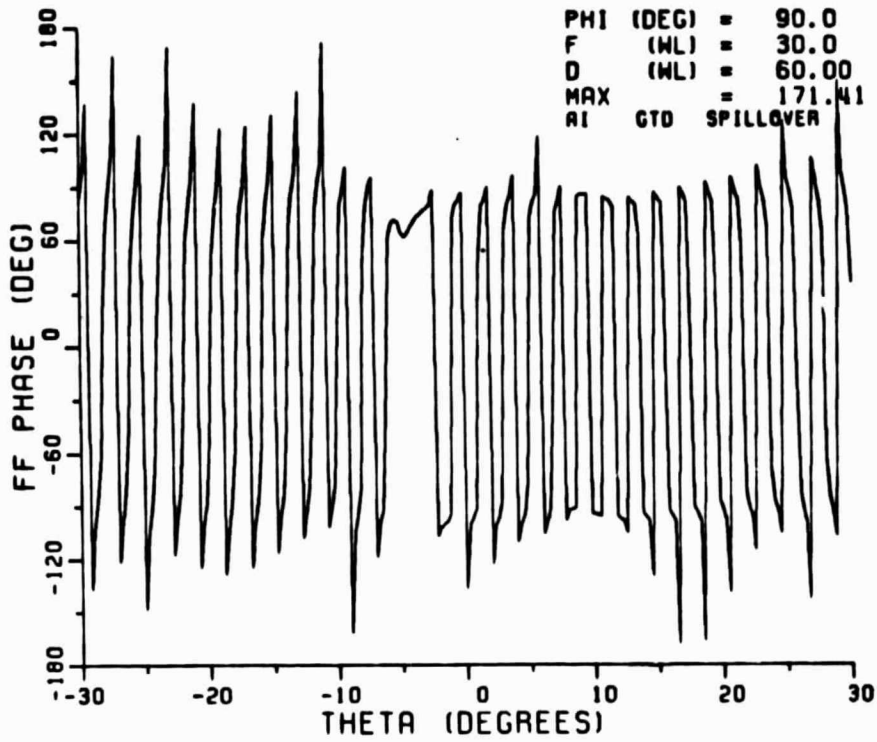


Figure 34. Phase of the radiated field in the yz plane when the feed is $(-0.5\lambda, 2\lambda, 0.)$ away from the focus.

Thus, one can use two feeds located at these two locations with a feedback loop. Since these two feeds will steer the main beam in two different directions, the noise entering them will be relatively uncorrelated.

Figure 35 shows the output INR of a sidelobe canceller with one modified feedback loop. The main antenna output is the signal received by a feed located at the focus of the reflector antenna, described earlier in this report. Signals received by two offset feeds located at $(0.5\lambda, 2\lambda, 0.)$ and $(-0.5\lambda, 2\lambda, 0.)$ with respect to the focus are the two inputs to the feedback loop. The INR at an isotropic antenna is assumed to be -30 dB. The output INR is plotted vs. the interfering signal direction for various values of noise correlation in the feedback loop. The interference suppression increases with a decrease in noise correlation. The angular region in which the interference is suppressed also increases with a decrease in noise correlation.

Comparing the output INR in Figure 35 with that in Figure 29, one observes that the interference suppression obtained by using a pair of offset feeds is smaller than that obtained by using a single offset feed. However, in the case of a single offset feed, only internal thermal noise can be decorrelated by using two separate amplifiers. Thus, external noise in the feedback loop will be correlated and if external noise is dominant, which is normally true, the noise correlation factor, ρ , will be approximately equal to unity. Therefore, the interference suppression which can be obtained using one offset feed

ORIGINAL PAGE IS
OF POOR QUALITY

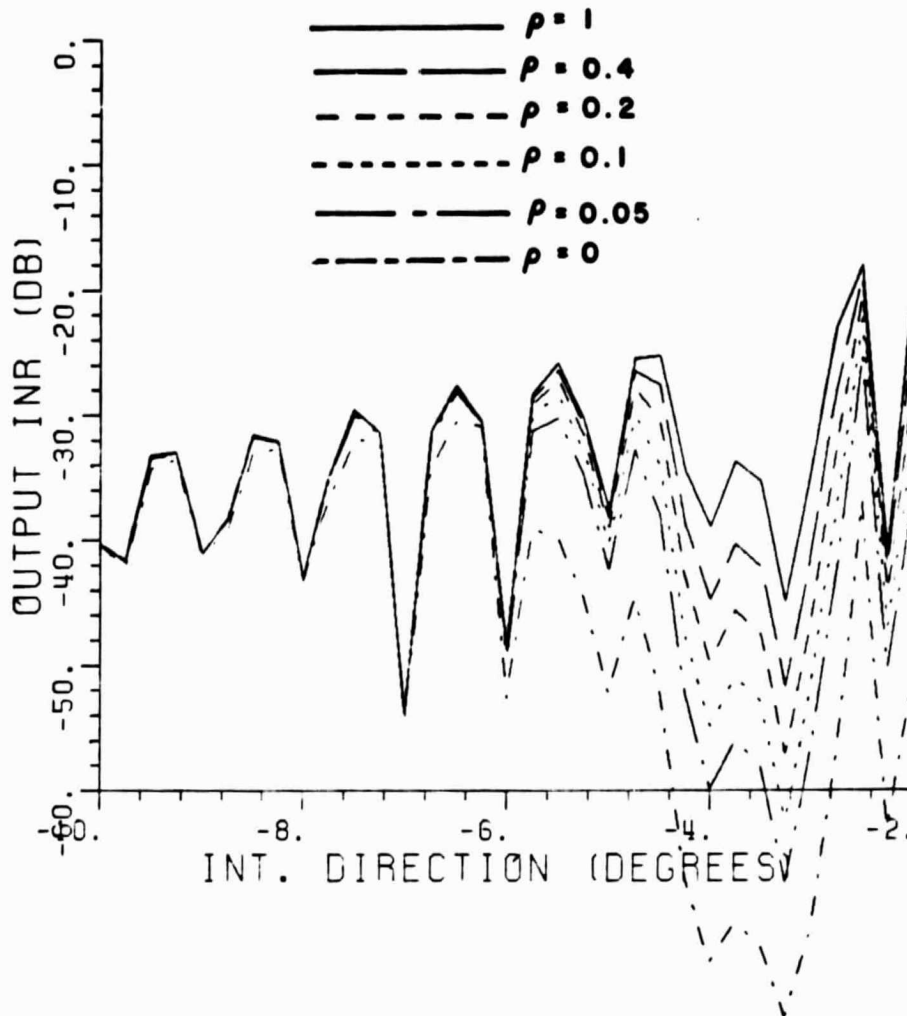


Figure 35. Output INR of a sidelobe canceller with one modified feedback loop vs. the interfering signal direction. A pair of offset feeds at $(\pm 0.5\lambda, 2\lambda, 0.)$, INR (isotropic) = -30 dB, $G/\alpha = 100$.

for each feedback loop corresponds to the ρ equal to unity curve in Figure 29. In the case of a pair of offset feeds, internal as well as external noise is decorrelated. Thus, noise correlation in the feedback loops will be approximately zero. In practice, ρ may be of the order of 0.05-0.1. For these values of ρ , the interference suppression obtained by using a pair of offset feeds is significantly higher than that obtained by a single offset feed ($\rho = 1$ plot in Figure 29). Thus, a pair of offset feeds can be used very effectively to increase the interference suppression.

The reason for the decrease in the interference suppression (for the same values of ρ in Figures 29 and 35) in the case of a pair of offset feeds is that by moving the offset feeds out of the yz plane, the main beam of the reflector antenna has been moved out of the yz plane. Thus, the gain of the auxiliary antennas in the direction of the interfering signal has decreased. Since the interference suppression decreases with a decrease in the INR in the auxiliary antennas [7], the interference suppression decreases. Figures 36 and 37 show the radiation patterns of the reflector antenna in the yz plane ($\phi = 90^\circ$) when the feed is located at $(0.5\lambda, 2\lambda, 0.)$ and $(-0.5\lambda, 2\lambda, 0.)$, respectively, with respect to the focus of the reflector. Note that the maximum gain of the reflector is 36.5 dB, which is 8 dB below the gain of the reflector antenna when the feed is located at $(0., 2\lambda, 0.)$.

Figure 38 shows the output INR when the INR at an isotropic antenna is -40 dB. All other parameters are the same as in Figure 35. Again the interference suppression and the angular region in which the

ORIGINAL PAGE IS
OF POOR QUALITY

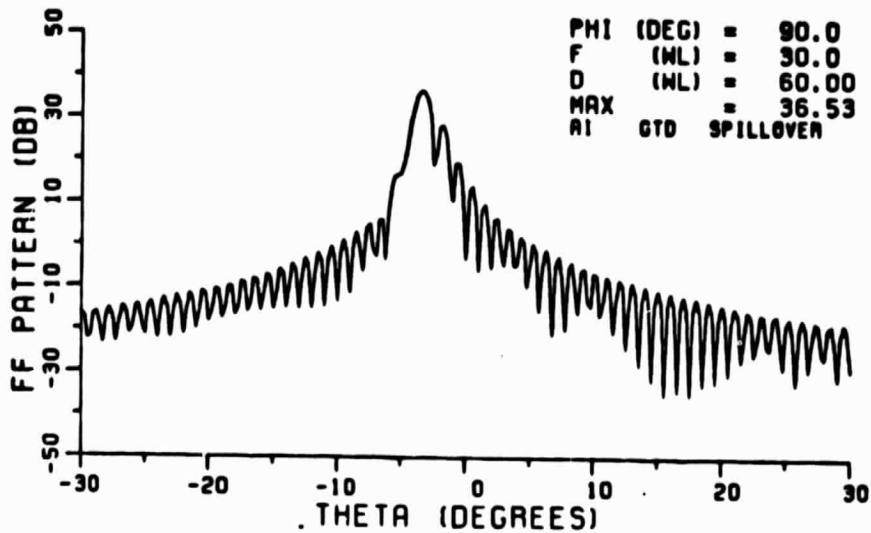


Figure 36. Radiation pattern of the antenna in yz plane when the feed is $(0.5\lambda, 2\lambda, 0.)$ away from the focus.

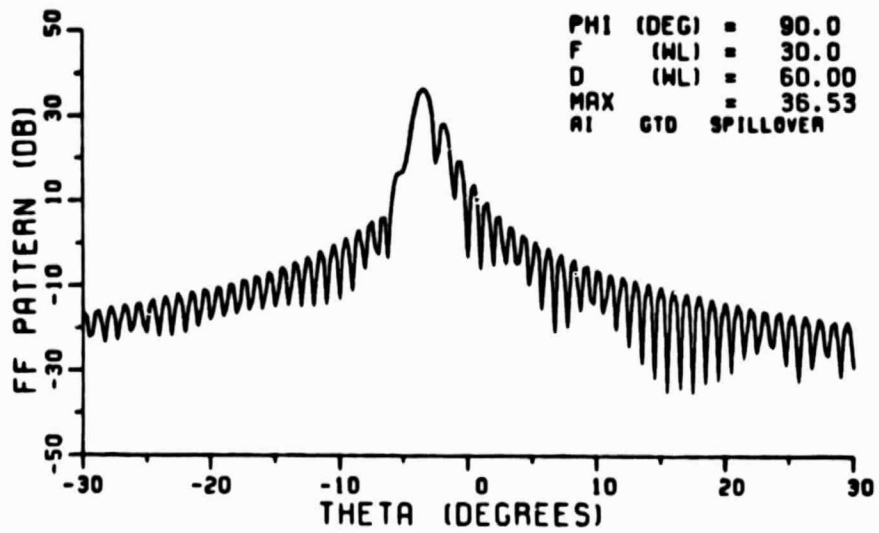


Figure 37. Radiation pattern of the antenna in yz plane when the feed is $(-0.5\lambda, 2\lambda, 0.)$ away from the focus.

ORIGINAL PAGE IS
OF POOR QUALITY

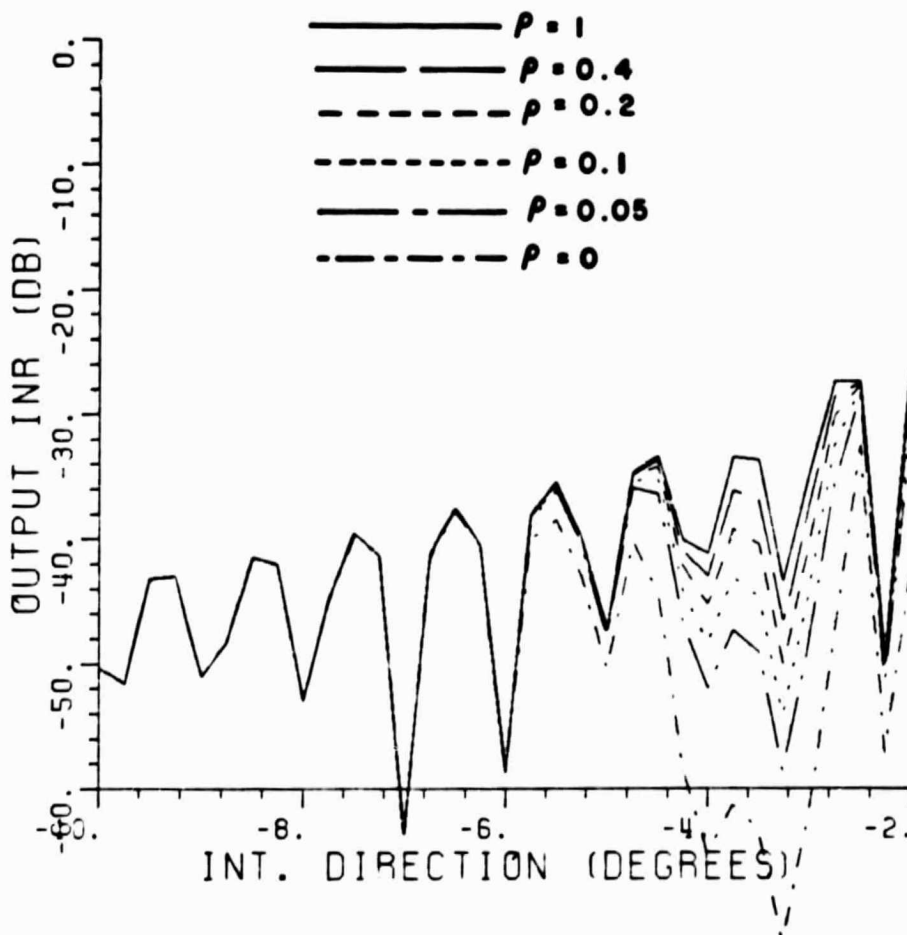


Figure 38. Output INR of a sidelobe canceller with one modified feedback loop vs. the interfering signal direction. INR (isotropic) = -40 dB. Other parameters are the same as in Figure 35.

interference is suppressed increases with a decrease in noise correlation. Comparing the plots corresponding to ρ less than 0.1 in this figure with ρ equal to unity in Figure 30, one can see that using a pair of offset feeds for each feedback loop, one can obtain higher interference suppression in spite of the drop in gain of the auxiliary antennas in the interfering signal direction.

In the above discussion, the interfering signal scenario consisted of a single interfering signal. It was shown that by using an offset feed of a reflector antenna as an auxiliary element of an adaptive array one can effectively suppress the interfering signal (if external noise is dominant, a pair of offset feeds should be used). The offset feed should be located such that the main beam of the reflector using this offset feed is in the general direction of the interfering signal. By using an array of offset feeds, one can similarly suppress multiple interfering signals. These offset feeds should be located such that the angular regions of the expected interference be covered by these offset feeds. For illustration, signal scenarios consisting of two interfering signals are considered next.

F. TWO INTERFERING SIGNALS

Figure 39 shows the INR at the output of the feed at the focus of the reflector antenna when the signal scenario consists of a desired signal and two interfering signals. The desired signal parameters are

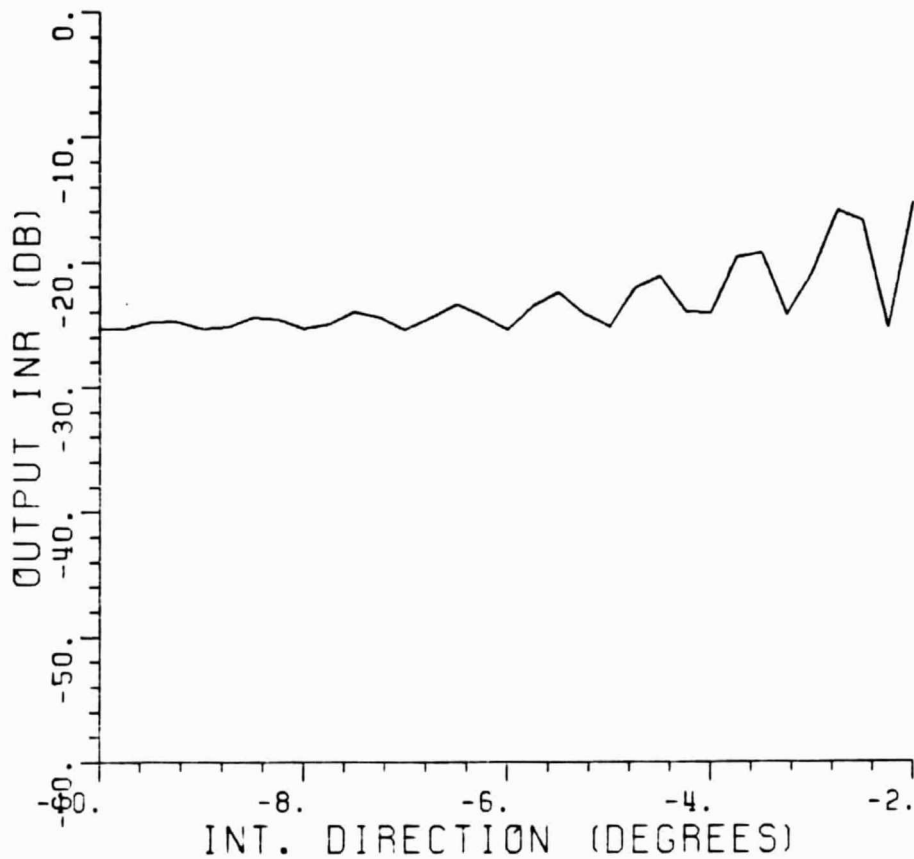


Figure 39. INR at the output of the feed at the focus vs. swept interference signal direction. Two interfering signals. $\theta_{i1} = 5.5^\circ$, INR (isotropic) for each interfering signal = -30 dB.

the same as before. The EIRP of the interfering signals are assumed such that the INR of each interfering signal at an isotropic antenna is -30 dB. One of the interfering signals is fixed and its angle of arrival is 5.5° (in yz plane) while the other interfering signal is swept between -10° and -2° . The output INR is plotted vs. the second interfering signal's direction. Comparing the INR in this figure with that in Figure 12, one can see that the INR in the presence of two interfering signals is significantly higher than in the presence of one interfering signal. The reason for this is that the fixed interfering signal is incident at the peak of a sidelobe of the center-fed reflector.

Figure 40 shows the output INR when an offset feed located at $(0., -3\lambda, 0.)$ with respect to the focus is used and the signal received by this feed is weighted adaptively and subtracted from the signal received by the feed at the focus (sidelobe canceller mode). All other parameters are the same as in Figure 39. The main beam of the reflector antenna using the offset feed is in the direction of the fixed interfering signal. Thus, the adaptive array should suppress this interfering signal. Comparing the output INR of the adaptive array with the INR in the main antenna in the presence of one interfering signal (Figure 12), one can see that the two are exactly equal. Thus, the interfering signal arriving from 5.5° has been suppressed by the adaptive array.

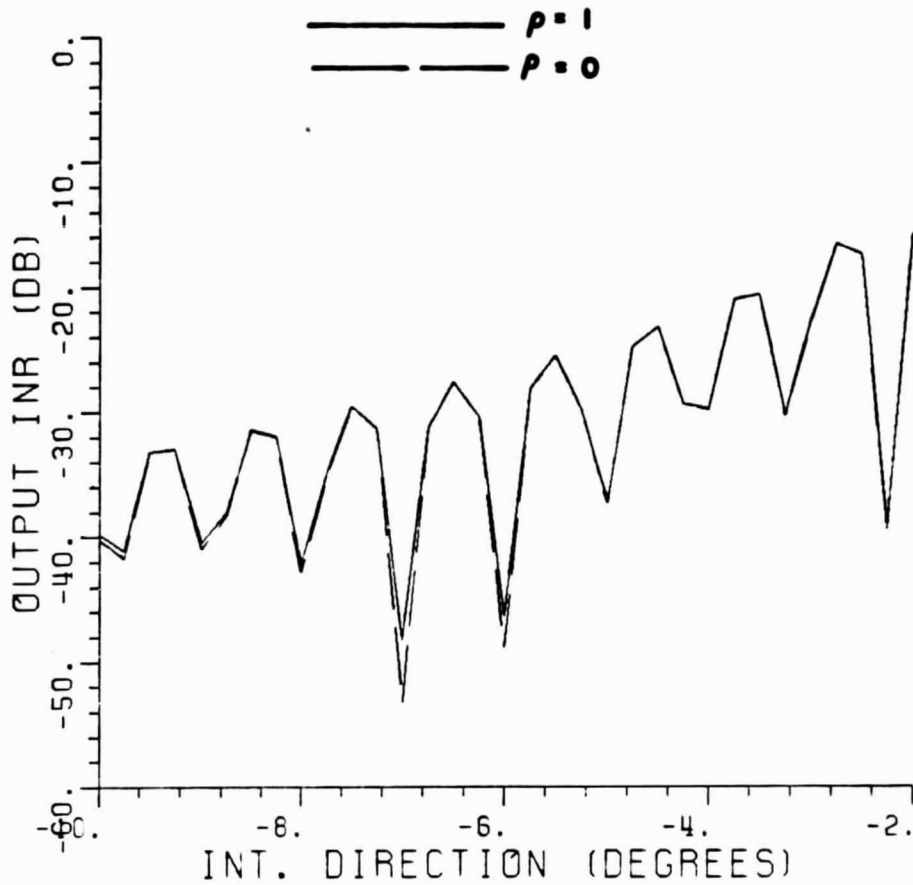


Figure 40. Output INR of a sidelobe canceller vs. the swept interference signal direction. One offset feed at $(0., -3\lambda, 0.)$. Two interfering signals $\theta_{i1} = 5.5^\circ$, INR (isotropic) for each interfering signal = -30 dB, $G/\alpha = 100$.

Figure 41 shows the output INR when another offset feed located at $(0., 2\lambda, 0.)$ with respect to the focus is used and the outputs of the two feeds are weighted adaptively using a sidelobe cancellation mode. The output INR is plotted for two values of noise correlation (ρ) in the feedback loops. Comparing the plots in Figures 40 and 41, one can see that when the angle of arrival of the swept interfering signal is between -4.8° and -2.4° , the output INR in the case of two offset feeds is smaller than that in the case of one offset feed. Thus, in this angular region the swept interfering signal is also suppressed by the adaptive array. The second offset feed has its main beam in this angular region [Figure 7]. Therefore, using two offset feeds, both interfering signals can be suppressed provided that the angular region of the interference sources are covered by the two feeds. Again the interference suppression and the angular region in which the interference is suppressed increases with a decrease in noise correlation in the feedback loops.

Figure 42 shows the output SINR of the sidelobe canceller. All parameters are the same as in Figure 41. The output SINR for all angles of arrival of the interfering signal is 14.5 dB, which is equal to the SNR of the output of the main antenna (feed at the focus). Thus, interferences are suppressed without any degradation in the SNR. In the above discussion, the two interfering signals were on the opposite sides of the desired signal. The situation where both interfering signals are on the same side of the desired signal is discussed next.

ORIGINAL PAGE IS
OF POOR QUALITY

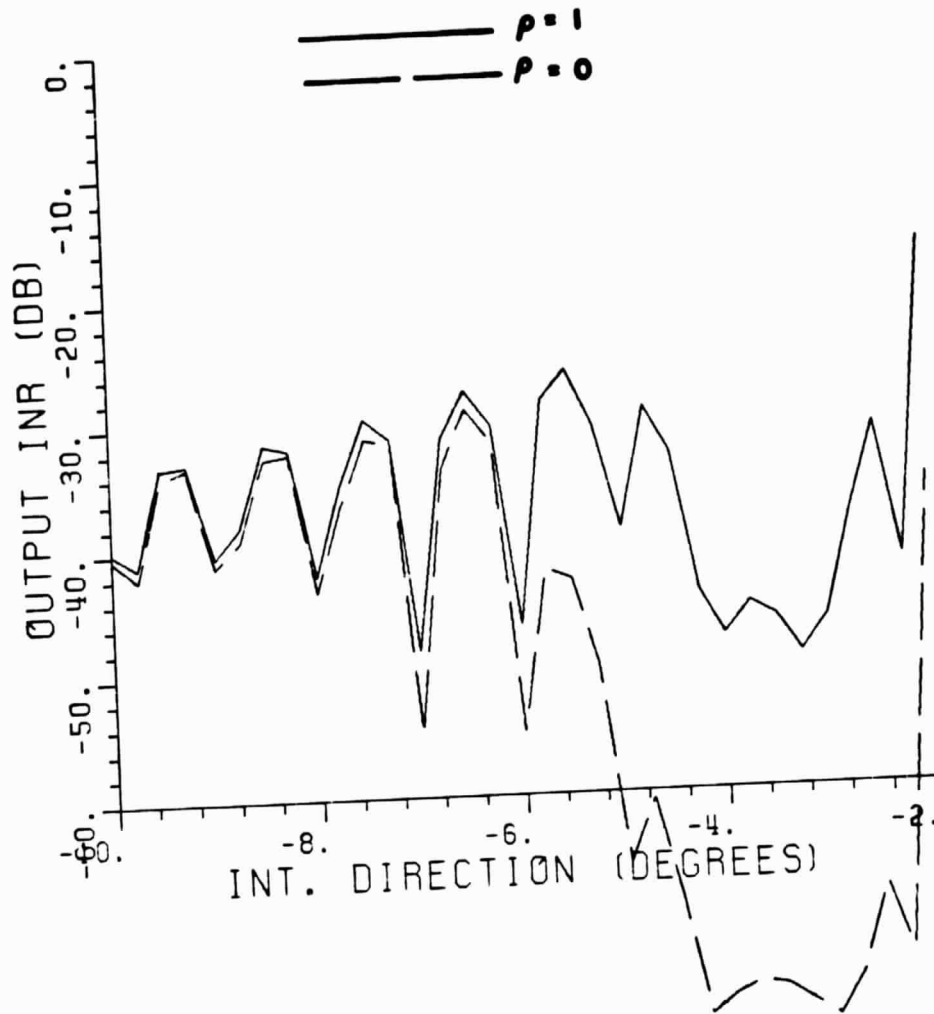


Figure 41. Output INR of a sidelobe canceller vs. the swept interference signal direction. Two offset feeds at $(0., -3\lambda, 0.)$ and $(0., 2\lambda, 0.)$, respectively. Other parameters are the same as in Figure 40.

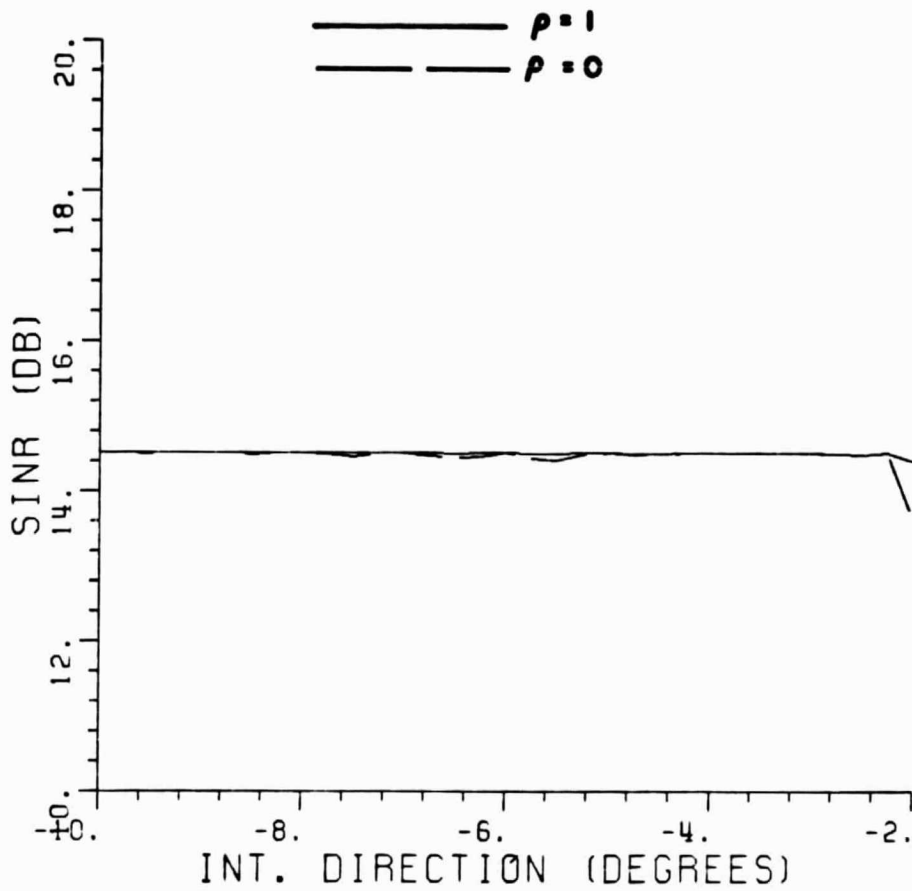


Figure 42. Output SINR of a sidelobe canceller vs. the swept interference signal direction. All parameters are the same as in Figure 41.

Figure 43 shows the INR at the output of the main antenna when the fixed interference signal is moved to -5.5° . All other parameters are the same as before. Comparing the INR in the figure with that in Figure 12, one can see that the INR in the presence of two interfering signals is significantly higher than in the presence of one interfering signal. The reason for this is that the fixed interfering signal is incident at the peak of a sidelobe of the main antenna.

Figure 44 shows the output INR of the sidelobe canceller with one offset feed. The offset feed is located at $(0., 3\lambda, 0.)$ with respect to the focus of the reflector. This offset feed steers the mainbeam of the reflector antenna to -5.5° . Thus, the sidelobe canceller should suppress the fixed interfering signal. Comparing the INR plots in Figures 44 and 12, one can see that for all angles of arrival of the swept interference, the output INR of the sidelobe canceller in the presence of two interfering signals is lower than the INR in the main antenna in the presence of one interfering signal. Thus, the fixed interference signal has been suppressed by the sidelobe canceller. When the swept interference is incident from -5.5° , the output INR of the sidelobe canceller is significantly smaller than the INR in the main antenna in the presence of one interfering signal. The reason for this is that both interference sources are in the same angular region and thus only one null in that angular region is enough to suppress both interfering signals.

Figure 45 shows the output INR when another offset feed located at $(0., 2\lambda, 0.)$ with respect to the focus is added to the sidelobe

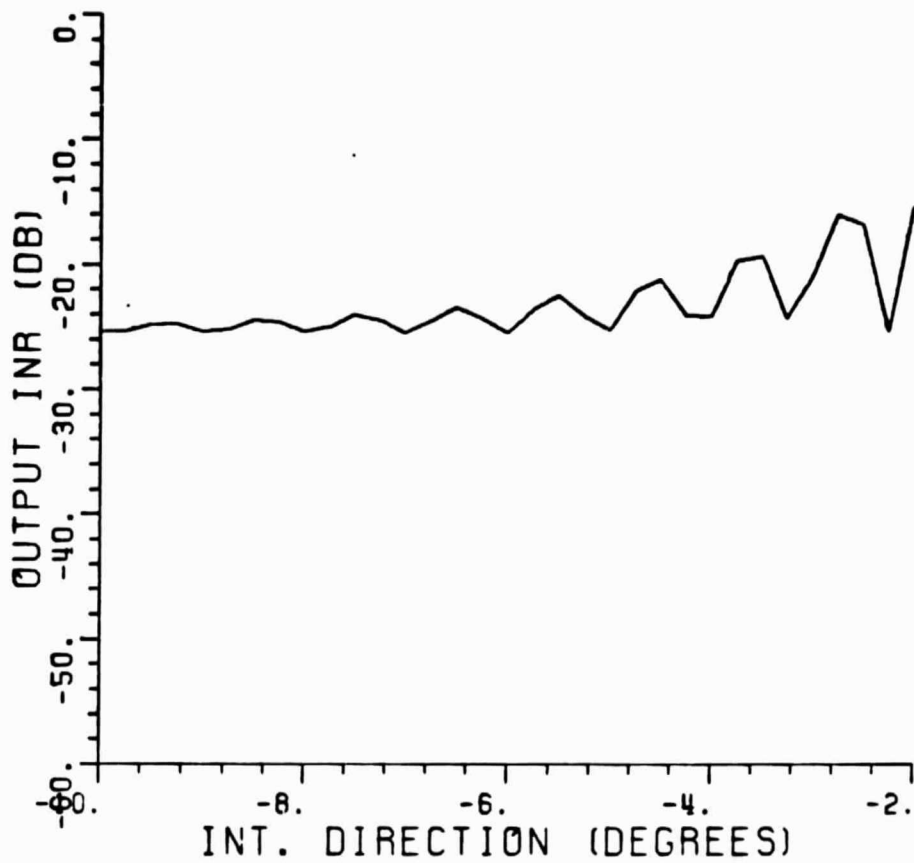


Figure 43. INR at the output of the feed at the focus vs. the swept interference signal direction. Two interfering signals. $\theta_{i1} = -5.5^\circ$, INR (isotropic) for each interfering signal = -30 dB.

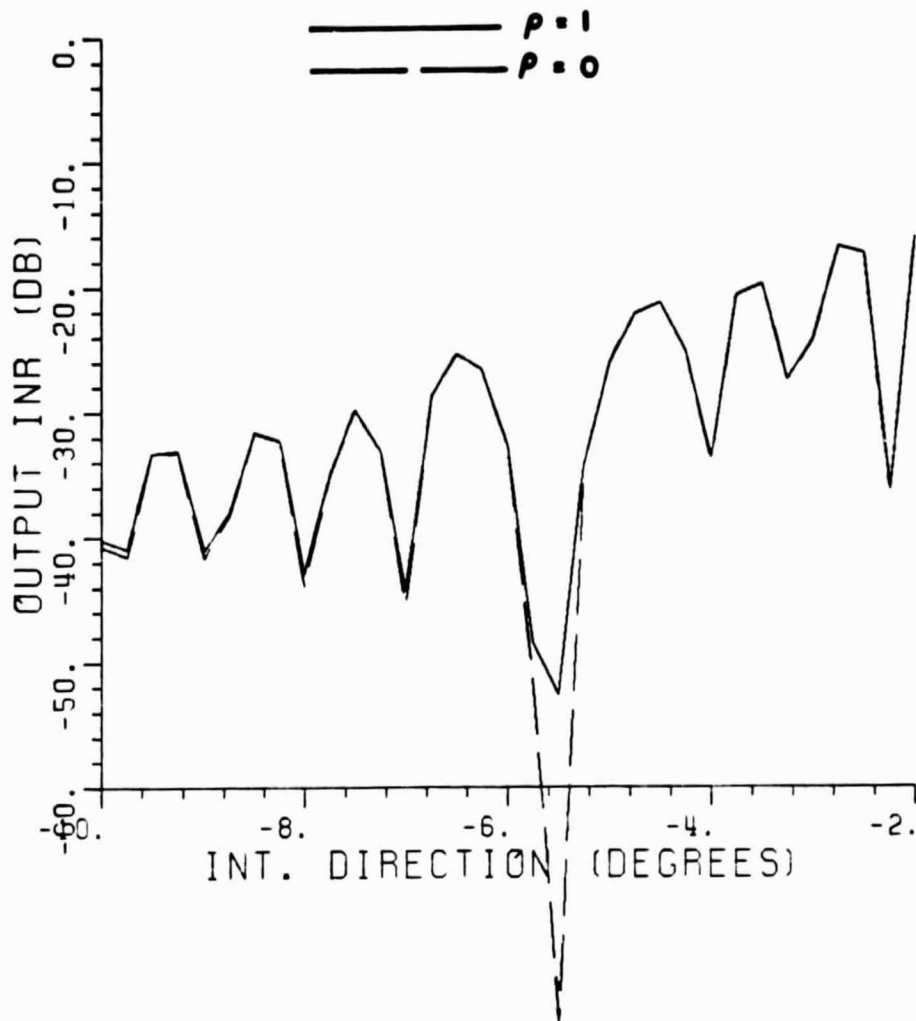


Figure 44. Output INR of a sidelobe canceller vs. the swept interference signal direction. One offset feed at $(0., 3\lambda, 0.)$. Two interfering signals, $\theta_{i1} = -5.5^\circ$, INR (isotropic) each interfering signal = -30 dB, $G/\alpha = 100$.

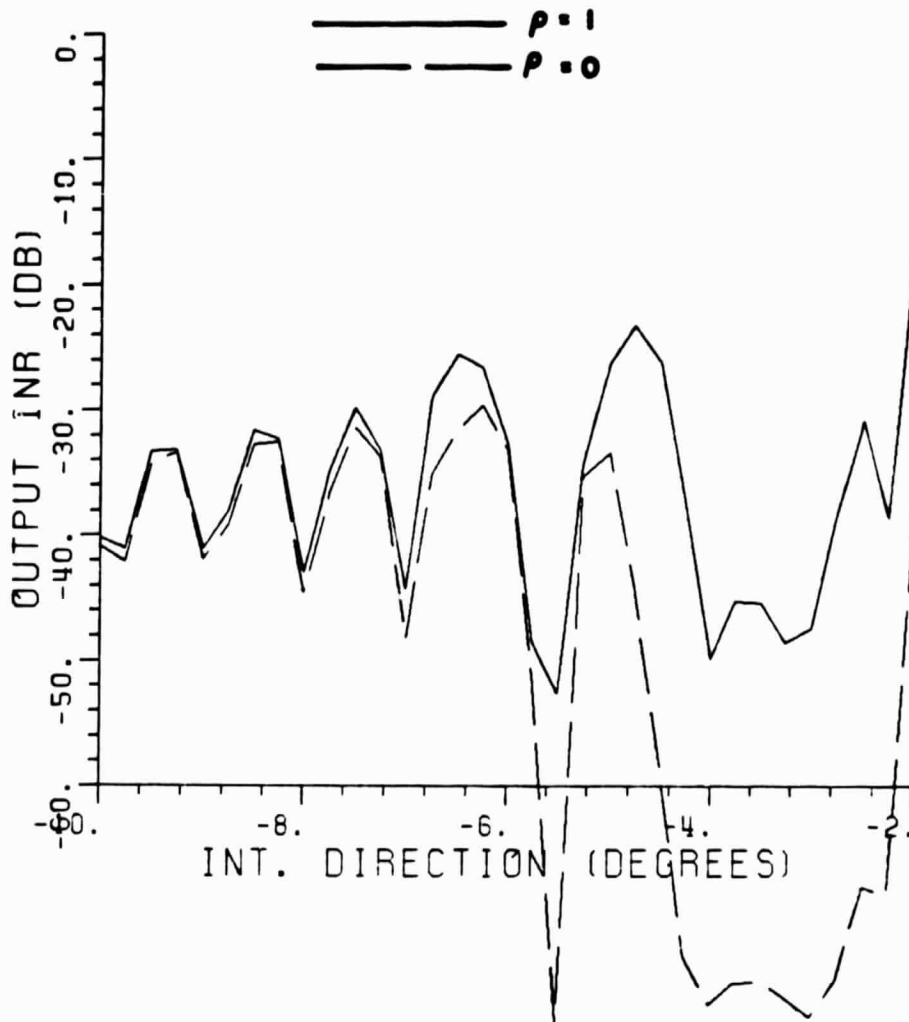


Figure 45. Output INR of a sidelobe canceller vs. the swept interference signal direction. Two offset feeds at $(0., 2\lambda, 0.)$ and $(0., 3\lambda, 0.)$. All other parameters are the same as in Figure 42.

canceller. Thus, there are two auxiliary antennas. All other parameters are the same as before. Comparing the plots in this figure with those in Figure 44, one can see that the angular region in which the swept interference is suppressed has increased. Now the second interference is suppressed even when it is incident between -4.4° and -2.6° . This is because the offset feed located at $(0., 2\lambda, 0.)$ steers the main beam of the reflector antenna in this direction. Again the interference suppression and the angular regions in which the interferences are suppressed increase with a decrease in noise correlation in the feedback loops.

Figure 46 shows the output SINR of the sidelobe canceller. All parameters are the same as in Figure 45. The output SINR for all angles of arrival of the swept interference is approximately 14.5 dB, which is equal to the SNR of the output of the main antenna. Thus, interferences are suppressed without adversely affecting the SNR. Hence two offset feeds of a reflector antenna can be very effectively used to suppress weak interfering signals provided that the angular region from which the interfering signals arrive are covered by the two beams obtained using the two offset feeds. Similarly, M offset feeds or offset feed pairs (if external noise decorrelation is required) can be used to suppress M interfering signals.

In this section, the performance of adaptive antennas was studied when offset feeds of a reflector antenna were used as auxiliary elements. It was shown that when the directions of sources of interference are known approximately, offset feeds can be used very

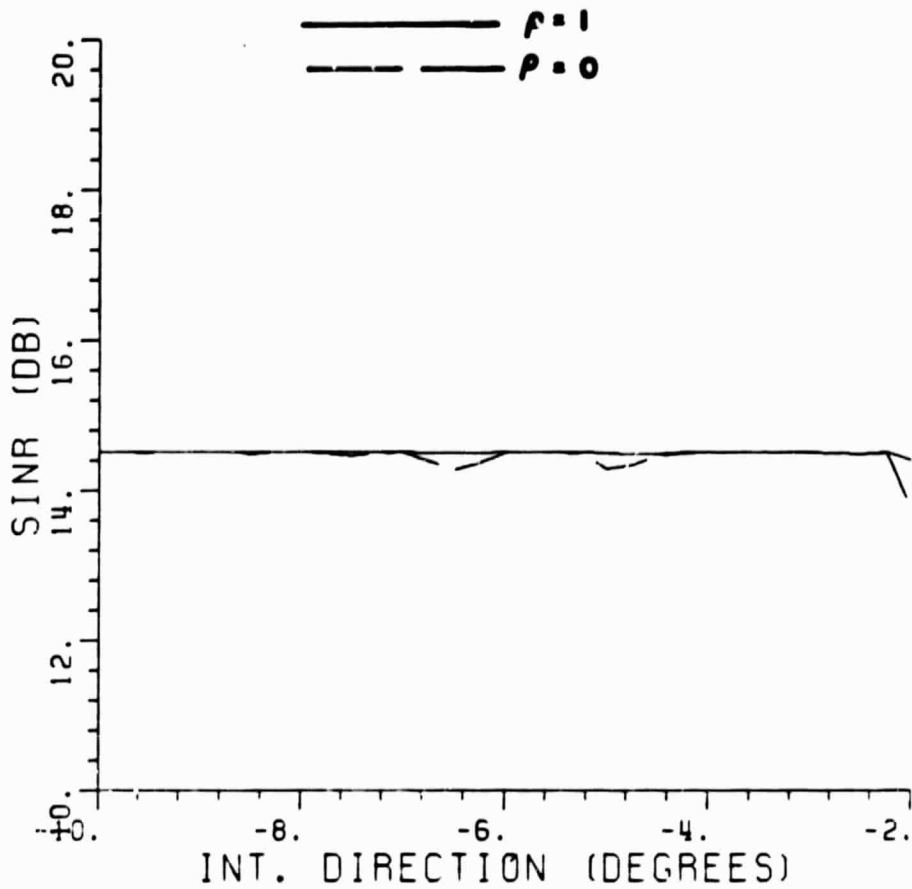


Figure 46. Output SINR of a sidelobe canceller vs. the swept interference signal direction. All parameters are the same as in Figure 45.

effectively to suppress weak interfering signals. An experimental system has been designed to verify the theoretical analysis. A detailed description of the experimental system and various tests which will be executed to verify the analytical work are discussed next.

IV. EXPERIMENTAL SYSTEM

A. INTRODUCTION

An experimental system has been designed to demonstrate the capabilities of adaptive antenna arrays in suppressing weak interfering signals and to determine the performance limit which can be achieved in practical applications. The system operates at 70 MHz and has a bandwidth of 6 MHz, representing a typical television channel. It is a sidelobe canceller with two auxiliary elements. Modified feedback loops are used to control the weights of the auxiliary channels. Two separate antennas displaced from each other are used with each feedback loop to reduce noise correlation. Thus, the total number of antenna elements in the array is five. Figure 47 shows a block diagram of the experimental system. It consists of an array simulator and an array processor. The signals received by the various antennas are generated in the array simulator. The array processor computes the complex weights which multiply the signals received by the auxiliary antennas to yield the array output. Details of the signal scenarios, the array simulator and the array processor are given below.

B. SIGNAL SCENARIOS

A typical scenario of current interest is that of a ground station receiving a television signal from a communication satellite in a geo-synchronous orbit. The location of this satellite is assumed to be

ORIGINAL PAGE IS
OF POOR QUALITY

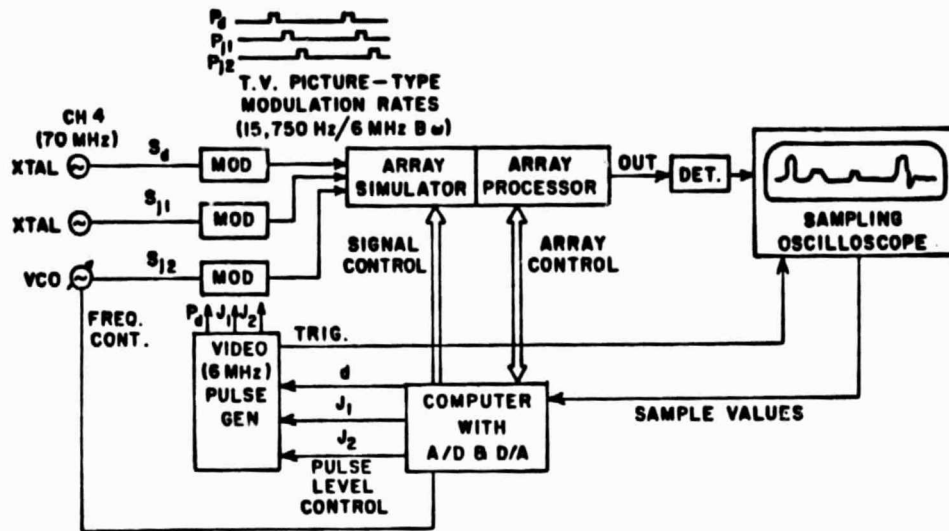


Figure 47. Block diagram of the experimental system.

known exactly so that desired signal tracking is not a requirement. The signal from this satellite (desired signal) is received by a high gain antenna. This antenna also receives some undesired signals through its sidelobes. The spectral characteristics and modulation of the undesired signals are assumed to be similar to that of the desired signal. The undesired signals are transmitted by other satellites in geosynchronous orbits. These satellites may be serving the same geographical area. Thus, the EIRP of the desired signal and the undesired signals may be approximately equal. However, because of the directivity of the ground station antennas, the signal-to-interference ratio in the receiver is 20-30 dB[†]. The signal-to-noise ratio in the receiver is assumed to be of the order of 13-16 dB. Thus, at times the interference may be well below the thermal noise level. Although weak, these signals because of their coherent nature and their similarity to the desired signal, do cause objectionable interference (i.e. ghosts) and must be further suppressed by up to 30 dB.

In the experimental system (Figure 47), the signal scenarios consist of three signals. One desired signal (S_d) and two interfering signals (S_{j1} and S_{j2}). The locations of the sources of interference are arbitrary and may vary (slowly) with time. The details of the antenna configuration used to receive these signals is discussed next.

[†]The ground station antenna is assumed to have -20 dB sidelobes (compared to the peak of the main beam). However, since the undesired signals may not be incident at the peak of a sidelobe, the signal-to-interference ratio in the receiver is 20-30 dB.

C. ANTENNA CONFIGURATION

The antenna is a five element array consisting of a high gain main antenna and two auxiliary element pairs. The array elements could be separate directional elements or separate feeds of a common reflector or beams of a steerable multiple beam array. The element distribution is shown in Figure 48. The signal source distribution is also shown in the figure. In this figure, D is the desired signal and J_1 and J_2 are two interfering signals. All the signals are assumed to be coplanar. The desired signal is received by a high gain antenna element (main antenna) at location 5. This element also receives undesired signals through its sidelobes. Antenna elements of moderate directivity at locations 1 and 2 are pointed in the general direction of the undesired signal J_1 while antenna elements at locations 3 and 4 look in the general direction of J_2 . Thus, the interference-to-noise ratio (INR) in these antenna elements (auxiliary antennas) is higher than that in the main antenna. Elements 1, 2, 3 and 4 will receive some desired signal through their sidelobes. Elements 1 and 2 will also receive some interfering signal J_2 . Similarly elements 3 and 4 will receive some interfering signal J_1 . Elements 1 and 2 are located symmetrically along a line perpendicular to the plane containing the signal sources. Thus, the phases of the three signals received by element 1 are exactly equal to the phases of the corresponding three signals received by element 2. However, because of their spatial separation, the sky noise in the two antenna elements will be only partially correlated. The same is true for elements 3 and 4.

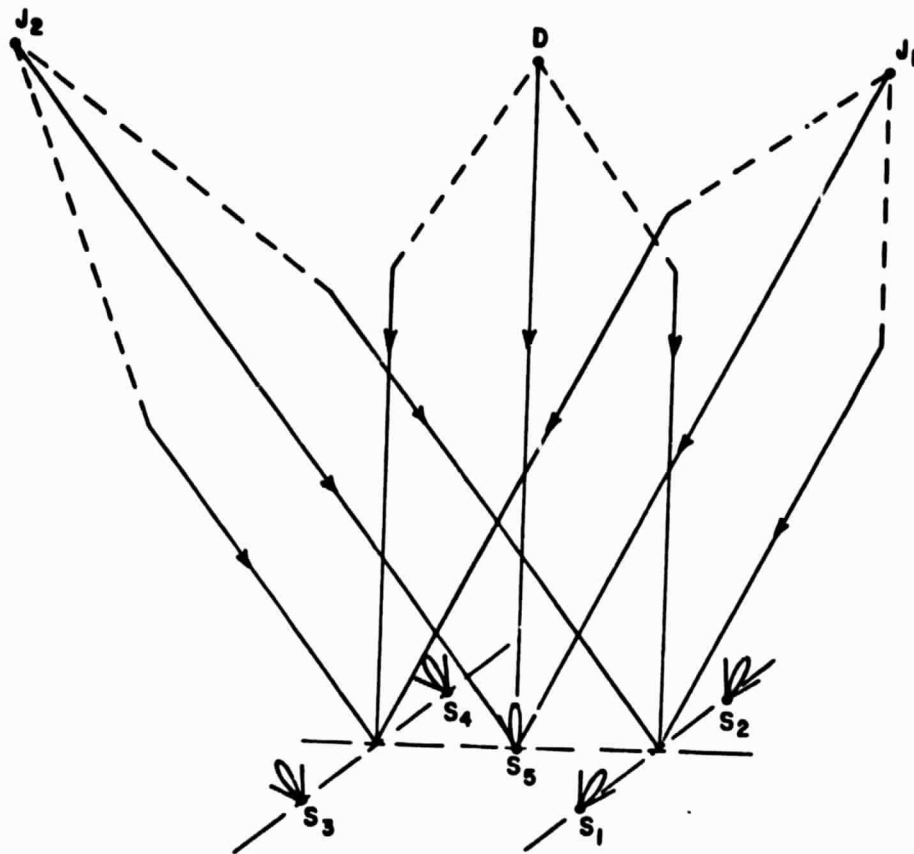


Figure 48. Distribution of array elements for the experiment.

In the current experiment, we will not be using actual antenna elements, although these could be added later, if desired. In the experiment, the signals that would have been received by the various antenna elements are synthesized to represent the various signal scenarios. This permits the evaluation of the adaptive array performance for various signals considered in the theoretical study. Details of the array simulator are discussed next.

D. ARRAY SIMULATOR

A simplified block diagram of the array simulator is shown in Figure 49. The three input signals, the desired signal and two interfering signals, are combined with uncorrelated noise inputs and fed to the output summing junctions to generate the signals received by the various antennas. Note that the thermal noise N_1 in the correlator branches* of the auxiliary channels is uncorrelated with the thermal noise in the signal branches*. The three signals in the correlator branches, however, are fully correlated with the corresponding three signals in the signal branches. Since the correlator inputs do not contribute to the array output, the same noise source (N_2) is used in the two correlator branches.

*The correlator branches correspond to the Y_i s in Figures 31 and 32 and the signal branches correspond to the x_i s.

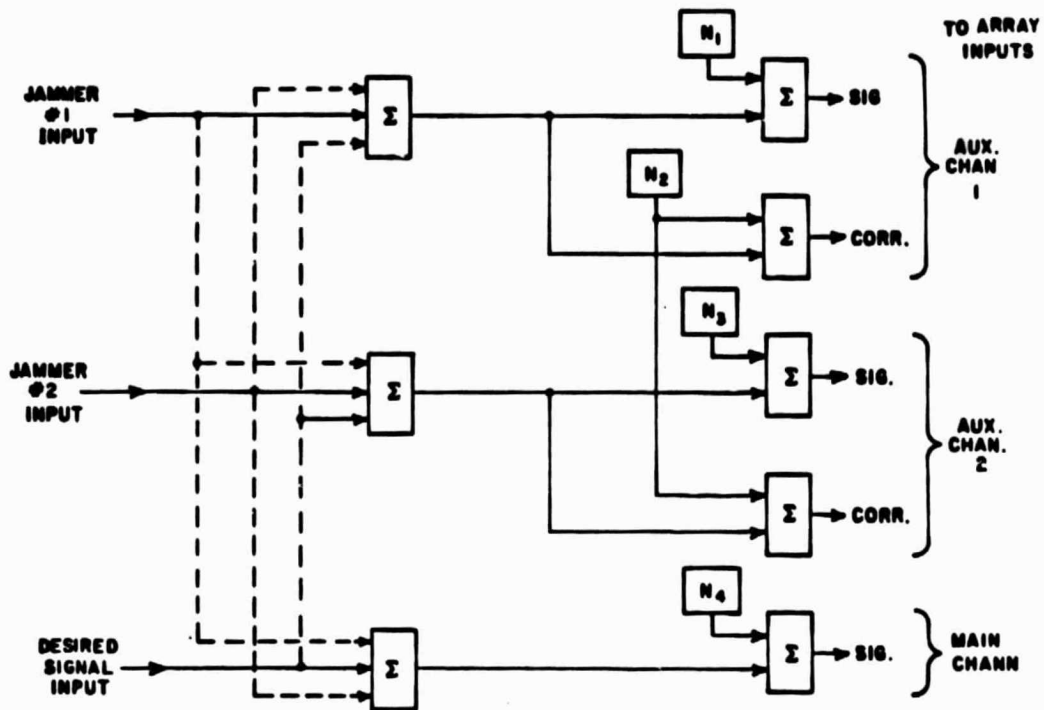


Figure 49. Array simulator.

Figure 50 shows the complete schematic diagram of the signal simulator except for details of the noise sources, N_1 to N_4 . The Δ 's in this figure are commercial (SMA connectorized) in-phase power dividers and the Σ 's are summing junctions (which are also implemented with in-phase power dividers, connected as summers). The α 's are adjustable attenuators and the ϕ 's are variable phase shifters.

The input attenuators, α_1 , α_2 and α_3 , used to control the signal levels of various signals, should be programmable to facilitate running data curves under computer control. The phase shifters, ϕ_1 , to ϕ_4 , which permit setting (and varying) the effective angle of arrival of the undesired signals, could also be programmable, if desired. Thus, the movements of the undesired signal sources can be simulated. High resolution programmable phase shifters are, however, quite expensive. Since in the current application, these movements are very slow, manually adjustable phase shifters could be used with little loss other than the operator's convenience. The attenuators, α_4 , α_5 , and α_6 , similarly could be manually adjustable types unless full programmability is desired for possible future applications.

The schematic diagram of a noise source is given in Figure 51. It consists of a reverse breakdown broadband noise diode followed by a variable gain amplifier. As shown, the amplifier gain and consequently the output noise level is voltage controlled and adjustable via a potentiometer. The output noise power could also be controlled by

ORIGINAL PAGE IS
OF POOR QUALITY

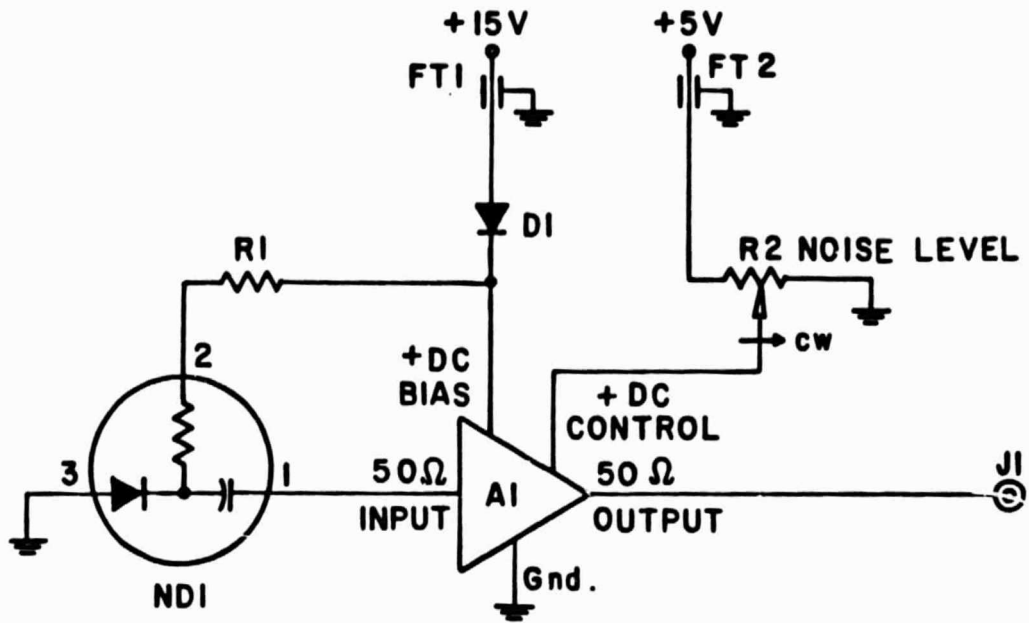


Figure 51. Schematics of a noise source.

computer, if desired, by replacing the +5V input by the output of a suitable D/A convertor and adjusting R_2 to obtain the desired maximum output.

E. ARRAY PROCESSOR

A block diagram of the array processor is given in Figure 52. It is a sidelobe canceller with two auxiliary channels. The two auxiliary channel signal inputs are analog weighted (both in phase and amplitude) by the vector modulators and are then summed with the main channel signal to form the array output. The correlator branch signals of the two auxiliary channels are down converted to base band and quadrature detected by the vector detectors. Part of the output signal is similarly detected to form the feedback error. The resulting base band voltages are simultaneously sampled, A/D converted and applied to the digital processor which implements the feedback algorithm for each of the two loops. The resulting digital weight vectors are D/A converted and applied as I and Q weight input voltages to the vector modulator.

In the proposed experimental system a digital processor is used to implement the feedback algorithm. The digital processor will perform the correlation between the array output and the individual antenna element and will update the array weights. By utilizing a digital processor, many problems often encountered with analog loops, especially at low signal levels, are avoided. These include effects of d.c.

ORIGINAL PAGE IS
OF POOR QUALITY

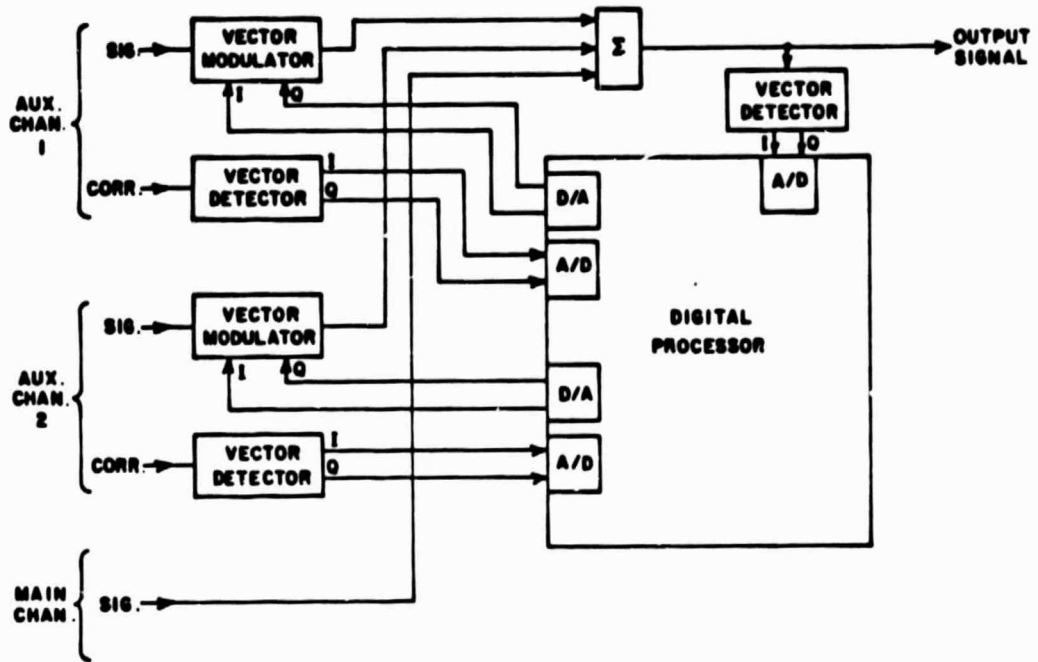


Figure 52. Array processor.

offsets, stray coupling and feedthrough associated with the correlator multiplier and leakage and d.c. offset in analog integrators. Also, the digital processor provides great flexibility in implementing various adaptive array algorithms without many hardware changes, which is very desirable in an experimental system. Thus, the performance of various adaptive algorithms can be studied and the effects on the array performance of various error sources such as steering vector errors can be evaluated.

A schematic diagram of the array processor is given in Figure 53. The input signals are first conditioned by bandpass filtering to the 6 MHz bandwidth of a conventional television signal. The center frequency is chosen as 69 MHz which permits readily available, economical and reliable 70 MHz IF components to be used. It also permits the use of channel 4 television signals for qualitative video testing. Variable gain IF amplifiers are provided to amplify the input signal levels, which may range from approximately -70 dBm to -30 dBm, to the level needed by the array processor (approximately 0 dBm). Test ports are provided at the IF output to permit convenient monitoring of the various array input signals.

The auxiliary channel signals are weighted via the vector modulators (VMOD-1 and VMOD-2) and are summed with the main channel signal as described before. The only change in this part of the circuit, relative to the simplified block diagram, is the addition of a programmable attenuator, α_1 , in the main channel. It permits computer

ORIGINAL PAGE IS
OF POOR QUALITY

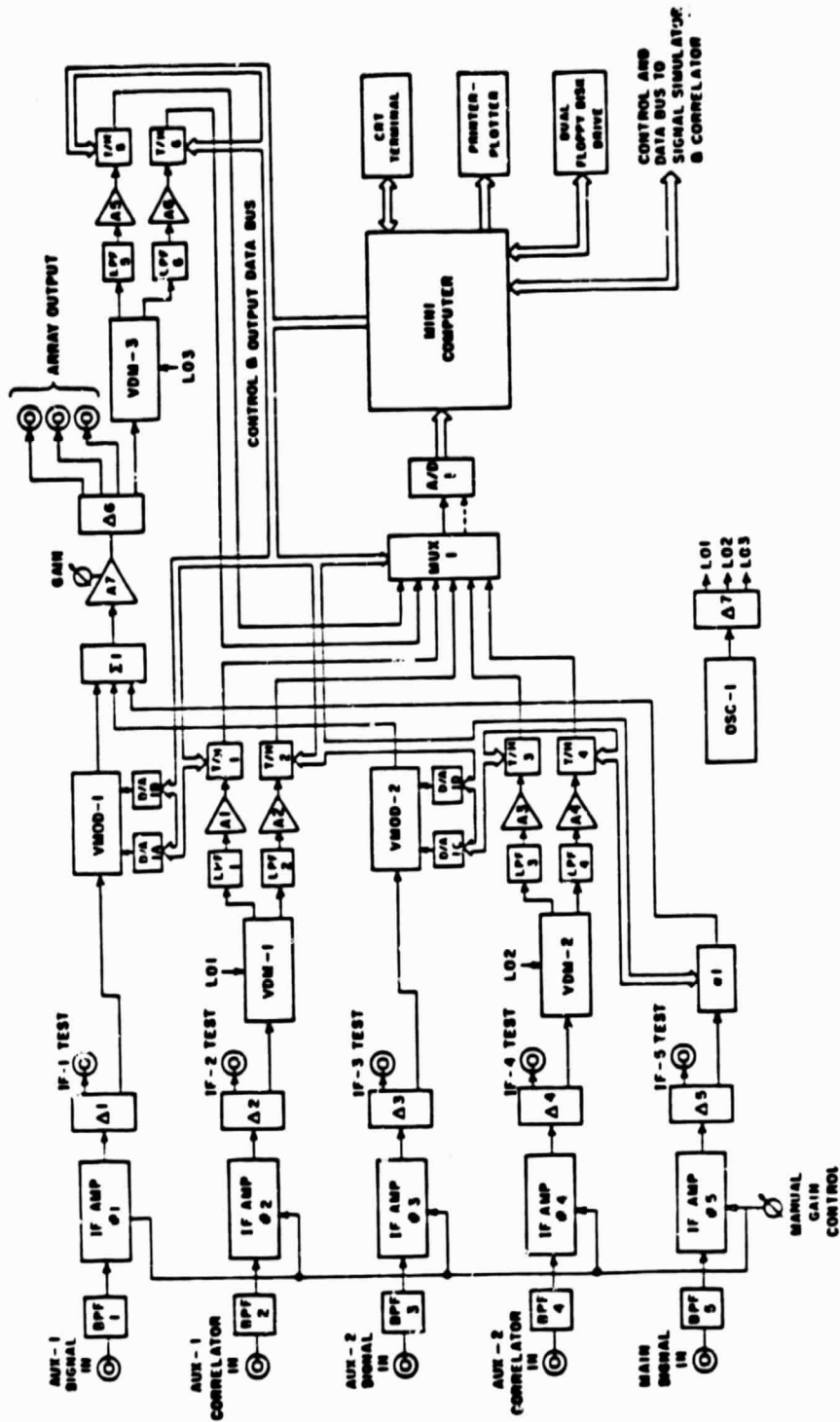


Figure 55. Detailed description of the array processor.

control of the main channel signal level. After summing, additional gain is provided by the variable gain amplifier, A_7 . The gain of this amplifier is set for best overall performance and dynamic range. The weights are calculated, serially, by the minicomputer using the desired programmed algorithm and are then sent to the proper D/A converters proceeding to the vector modulator I and Q inputs. Each new weight is stored in an input register (an integral part of the D/A converter chip) as it is generated, but is not applied until all the weights are computed. At that time all of the new weights are transferred to an output storage register (also an integral part of the D/A converter chip) by computer command and the new analog weights are generated to update the vector modulator I and Q weight inputs.

It is expected that a standard laboratory mini-computer (a PDP11/23 is currently available at the ElectroScience Laboratory) will be used for digital implementation of the feedback algorithms as well as for parameter control, experimental data recording and data analysis. For the currently proposed experiment, the five inputs to the array processor are obtained using the array simulator described in subsection C. Later, if desired, the same array processor could be used with actual antenna elements whose signals are down converted to 70 MHz and preamplified and fed to the array processor. Thus, the experimental set-up can be used with real systems. We are proposing to build the experimental system and execute a series of tests to verify the analytical work. Various tests which will be executed are discussed next.

F. EXPERIMENTAL VERIFICATION AND TESTING

The experimental system will be used to test the performance of various adaptive array algorithms qualitatively as well as quantitatively. The qualitative tests will demonstrate the improvement in the picture quality of a television signal with the use of adaptive arrays. In the presence of interference, the television picture will deteriorate in quality. If the interference is incoherent or noiselike in nature, the overall clarity of the picture will suffer. If the interference is coherent, either due to multipath or another television signal, the distortion will be of the form of "ghost" or extraneous images. This kind of distortion is more annoying and is more easily detectable by a human observer. It is this kind of interference that imposes the requirements for very deep nulls in the pattern of the antenna or equivalently a very thorough suppression of the interfering signals to well below the noise level. It is, therefore, proposed that such signals be used to test the ability of the adaptive arrays to eliminate the weak interfering signals.

In order to measure quantitatively the adaptive array's ability to suppress weak interfering signals, the following tests are proposed. They are especially relevant to the type of interference mentioned above, namely "ghosts". In these tests, the desired signal is a carrier S_d whose envelope is modulated by a string of pulses P_d at the television picture horizontal scan rate as shown in Figure 47. The

interfering signals are likewise pulse amplitude modulated signals ($S_{ji} \times P_{ji}$). One of the interfering signals has a fixed carrier frequency offset by a fixed amount from the desired signal while the carrier frequency of the second interfering signal would be continuously variable. These pulses will be delayed by a quarter of the pulse repetition period from each other and from those of the desired signal. On the screen of a television, these undesired signals will appear as vertical lines (ghosts). The bandwidth of the pulses would correspond to the bandwidth of a television channel. The frequency of one of the signals as well as the amplitude of various pulses will be controlled by the system computer.

At the output of the array processor, the signal will be detected and delivered to a sampling oscilloscope. The computer will be able to read the data from the oscilloscope and thus will have data corresponding to the output of the array processor as a function of time. The system operator will be able to directly observe the output displayed in various formats depending on the processing option selected. The various processing options will be programmed in software once the hardware is implemented. To find the interference suppression, the relative amplitude of the undesired signal will be measured with respect to the desired signal at the output. The distortion of the various output pulses will be measured to find the desired signal distortion. In the oscilloscope cumulative mode, the effect of signal integration (or detector bandwidth) will be studied. A bit error rate

study will be performed by implementing various pulse detection algorithms at the expected location of the desired pulse, the undesired pulses, and "no-pulse" portion of the waveform.

It is particularly important to note that since the entire system is under computer control, it is possible to study the dynamics of the system. The computer can "freeze" the adaptive array algorithms at any portion of the adaptive process and measure the array parameters and the signal parameters at various points in the system. The implementation of the various parametric studies can be programmed into the system computer. Thus, a study of the effect of the variation of one parameter on the performance of another parameter can be implemented and the results automatically computed and displayed (as an example, consider a study of the leakage of S_{j1} through the array processor as a function of amplitude of S_{j1}). The present particular application of adaptive arrays to communication satellites, where a quasistationary environment prevails, provide a unique opportunity to utilize a digital processor for the array processing as well as a variety of other functions such as experimental parameter control, data recording, processing and display in real time with the opportunity of an interactive mode.

V. SUMMARY AND FUTURE WORK

The performance of adaptive antennas was studied for the case where offset feeds of a reflector are used as auxiliary elements. Adaptive antennas operating in a fully adaptive mode (steered beam adaptive arrays) as well as a sidelobe canceller were considered. It was shown that when the main antenna is a reflector antenna, one can use the offset feeds of the reflector as auxiliary elements of an adaptive array to achieve the desired interference suppression in the satellite communication systems under consideration. In such communication systems the interfering signals are very weak (below thermal noise level). To suppress such interfering signals, the auxiliary antennas should be directive and be steered in the general direction of the interfering signals [7] and the feedback loops controlling the array weights should be modified. In the modified feedback loops, the noise level in the feedback loops is reduced by reducing the correlation between the noise components of the two inputs to the correlators in the feedback loops. When the external noise is the dominant source of noise, which is normally true, two separate antennas should be used for each feedback loop to reduce noise correlation. The two antennas should be located such that the phase of the interfering signal in the two is the same while the noise in them is uncorrelated. It was shown that the offset feeds of a reflector can be used to meet the above requirements.

In the case of a reflector antenna, by moving the feed away from the focus of the reflector, one can steer the beam over a wide angular

region. Thus, by the proper selection of feed location, one can steer the main beam in the general direction of an interfering signal and by using an array of feeds, all signals (desired and undesired) can be received with high gain. One can also use two offset feeds, displaced from each other, for each feedback loop to achieve noise decorrelation. It was shown that the two feeds can be located such that the phase of the various signals in the two feeds is the same. Thus, all the above requirements can be met and the desired interference suppression can be obtained. We are proposing to do the same kind of study when the receiving antenna is an array of small antennas. The possibility of using sub-arrays of the main antenna as auxiliary elements will be studied. In this case, one may have to use additional antennas as auxiliaries. The radiation characteristics and spatial distribution of the auxiliary antennas will be determined. The interference protection provided by such antennas will be computed and compared with other antenna systems.

An experimental system has been designed to verify our theoretical analysis and determine the performance limits which can be achieved in practical applications. A detailed description of the experimental system and the various tests which will be executed to verify the analytical work were also presented in this report. Under an extension of the present grant, we are proposing to implement the experimental system and execute the various tests.

REFERENCES

- [1] P.W. Howell, "Intermediate Frequency Sidelobe Canceller", U.S. Patent 3,202,990, August 1965.
- [2] S.P. Applebaum, "Adaptive Arrays", Technical Report SURC TR66-1, August 1966, Syracuse University Research Corporation.
- [3] B. Widrow, P.E. Mantey, L.J. Griffiths and B.B. Goode, "Adaptive Antenna Systems", Proceedings of IEEE, Vol. 55, No. 12, pp. 2143-2159, December 1967.
- [4] C.L. Zahn, "Application of Adaptive Arrays to Suppress Strong Jammers in the Presence of Weak Signals", IEEE Transactions on Aerospace and Electronic Systems, Vol. AES-9, No. 2., pp. 260-271, March 1973.
- [5] R.T. Compton, Jr., R.J. Huff, W.G. Swarner and A.A. Ksienski, "Adaptive Arrays for Communication Systems: An Overview of Research at the Ohio State University", IEEE Trans. on Antenas and Propagation, Vol. AP-24, No. 5, pp. 599-607, September 1976.
- [6] I.J. Gupta and A.A. Ksienski, "Adaptive Arrays for Satellite Communications", Technical Report 716111-1, June 1984, The Ohio State University ElectroScience Laboratory, Department of Electrical Engineering, prepared under Grant NAG3-536 for NASA/Lewis Research Center, Cleveland, Ohio.
- [7] I.J. Gupta, "Adaptive Antenna Arrays for Weak Interfering Signals", Technical Report 716111-2, January 1985, The Ohio State University ElectroScience Laboratory, Department of Electrical Engineering, prepared under Grant NAG3-536 for NASA/Lewis Research Center, Cleveland, Ohio.
- [8] R.C. Rudduck and Y.C. Chang, "Numerical Electromagnetic Code-Reflector Antenna Code, Part I: User's Manual (Version 2)", Technical Report 712242-16 (713742), December 1982, The Ohio State University ElectroScience Laboratory, Department of Electrical Engineering, prepared under Contract N00123-79-C-1469 for Naval Regional Procurement Office.
- [9] Y.C. Chang and R.C. Rudduck, "Numerical Electromagnetic Code-Reflector Antenna Code, Part II: Code Manual (Version 2)", Technical Report 712242-17 (713742), December 1982, The Ohio State University ElectroScience Laboratory, Department of Electrical Engineering, prepared under Contract N00123-79-C-1469 for Naval Regional Procurement Office.

APPENDIX A

In this section, the correlation between the noise entering two antennas, displaced from each other, is studied. Isotropic as well as directive antennas are considered. It is shown that if the external noise is uniformly distributed across the visible range, complete noise decorrelation may be obtained from two isotropic antennas spaced half a wavelength apart. At any separation larger than half a wavelength, the noise correlation is relatively small and decreases as the separation increases. The noise decorrelation further decreases as the system bandwidth increases. In the case of directive antennas, it is shown that the two antennas may be pointed in different directions to decorrelate the noise. In this case, the noise entering the two antennas arrives from mostly different portions of the observation range and thus assures relatively small noise correlation. The noise correlation further decreases with spatial separation between two antennas. Noise correlation between two isotropic antennas is discussed first.

NOISE CORRELATION BETWEEN TWO ISOTROPIC ANTENNAS

Let the noise be uniformly distributed across the whole visible space and have a flat spectral density as shown in Figure A.1. Then the correlation between the noise entering two isotropic antenna (Figure A.2) displaced a distance 'd' from each other is

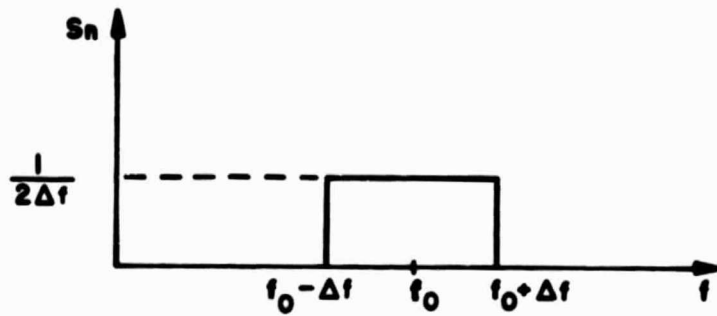


Figure A.1. Noise spectral density S_n .

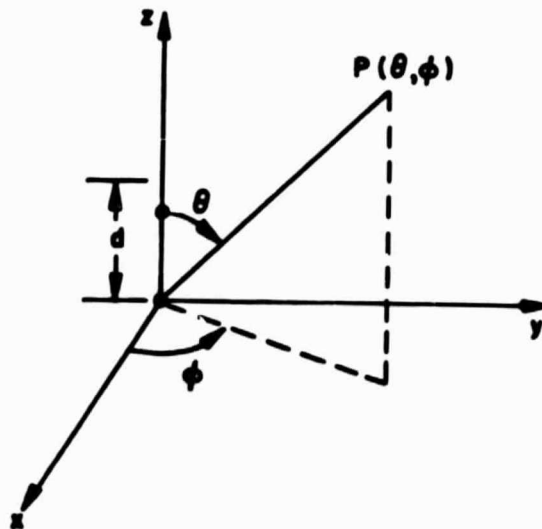


Figure A.2. Spatial distribution of two isotropic antennas.

$$\rho = \frac{1}{2\Delta f} \frac{1}{4\pi} \int_{f_0 - \Delta f}^{f_0 + \Delta f} \int_0^{2\pi} \int_0^{\pi} e^{jkdcos\theta} \sin\theta \, d\theta \, d\phi \, df \quad (A.1)$$

where f_0 is the centre frequency, $2\Delta f$ is the system bandwidth and k is the propagation constant,

$$k = \frac{2\pi f}{c} \quad (A.2)$$

where c is the velocity of light in free space and f is the frequency of electromagnetic wave. From (A.1)

$$\rho = \frac{1}{2\alpha\Delta f} \int_{f_0 - \Delta f}^{f_0 + \Delta f} \frac{1}{f} \sin(\alpha f) \, df \quad (A.3)$$

where

$$\alpha = \frac{2\pi d}{c} \quad (A.4)$$

Now

$$\int \frac{\sin \alpha f}{f} \, df = \alpha f - \frac{(\alpha f)^3}{3 \cdot 3!} + \frac{(\alpha f)^5}{5 \cdot 5!} - \dots \quad (A.5)$$

Substituting (A.5) in (A.4) one gets

$$f = 1 - \frac{\alpha^2 (3f_0^2 + \Delta f^2)}{3 \cdot 3!} + \frac{\alpha^4 (5f_0^4 + 10\Delta f^2 f_0^2 + \Delta f^4)}{5 \cdot 5!} - \dots \quad (A.6)$$

Let

$$d = s\lambda_0$$

then

$$\alpha = \frac{2\pi s\lambda_0}{c} = \frac{2\pi s}{f_0} = \frac{x}{f_0} \quad (\text{A.7})$$

where $x = 2\pi s$,

and λ_0 is the wavelength at the center frequency and s is the separation between two antennas at the center frequency. Substituting (A.7) in (A.6) one gets

$$\rho = 1 - \frac{x^2 (3 + (\frac{\Delta f}{f_0})^2)}{3 \cdot 3!} + \frac{x^4 (5 + 10 (\frac{\Delta f}{f_0})^2 + (\frac{\Delta f}{f_0})^4)}{5 \cdot 5!} \dots \quad (\text{A.8})$$

Collecting the terms with same powers of $\frac{\Delta f}{f_0}$, one gets,

$$\rho = \sum_{n=0}^{\infty} \frac{(-1)^n x^{2n}}{2n+1!} - \frac{x^2}{3!} \left(\frac{\Delta f}{f_0}\right)^2 \sum_{n=0}^{\infty} \frac{x^{2n} (-1)^n}{2n+3 \cdot 2n!} + \frac{x^4}{5!} \left(\frac{\Delta f}{f_0}\right)^4 \sum_{n=0}^{\infty} \frac{x^{2n} (-1)^n}{2n+5 \cdot 2n!} \dots \quad (\text{A.9})$$

For narrowband systems, $\frac{\Delta f}{f_0} \ll 1$, thus (A.9) can be approximated as

$$\rho = \sum_{n=0}^{\infty} \frac{(-1)^n x^{2n}}{2n+1} = \frac{\sin x}{x} \quad (\text{A.10})$$

$$= \frac{\sin(2\pi s)}{2\pi s}$$

A plot of ρ as given in (A.10) vs. s is shown in Figure A.3. Note that the noise correlation is zero for all separations corresponding to multiples of halfwavelength ($s = 0.5, 1, 1.5, 2$ -----). At any separation larger than half a wavelength, the noise correlation is relatively small and decreases as the separation increases.

For wideband systems, the noise correlation will be given by (A.9). A plot of (A.9) for various values of $\frac{\Delta f}{f_0}$ is given in Figure A.4. Note that the noise correlation for wideband systems ($\Delta f/f_0 \neq 0$) is less than for a CW system ($\Delta f/f_0 = 0$). The noise correlation for a given separation between two isotropic antennas decreases with an increase in the system bandwidth. The noise correlation between two directive antennas is studied next. Since, it has been demonstrated that noise correlation decreases with an increase in the system bandwidth, only CW systems are considered.

NOISE CORRELATION BETWEEN TWO DIRECTIVE ANTENNAS

In this section, correlation between noise entering two similar directive antennas is studied. Again, the external noise is assumed to be uniformly distributed across the visible range. It is shown that

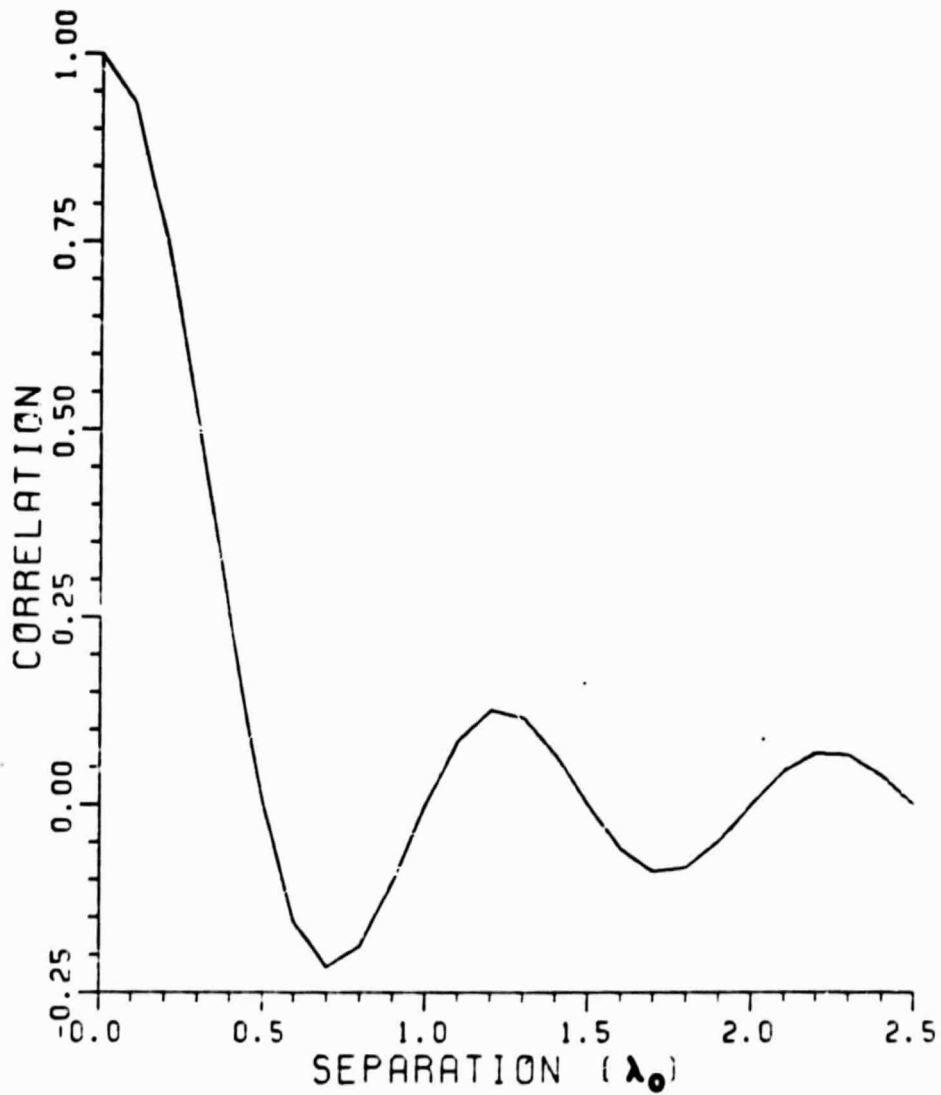


Figure A.3. Noise correlation between two isotropic antennas vs. the separation between antennas. System bandwidth is assumed to be zero, $\Delta f = 0$.

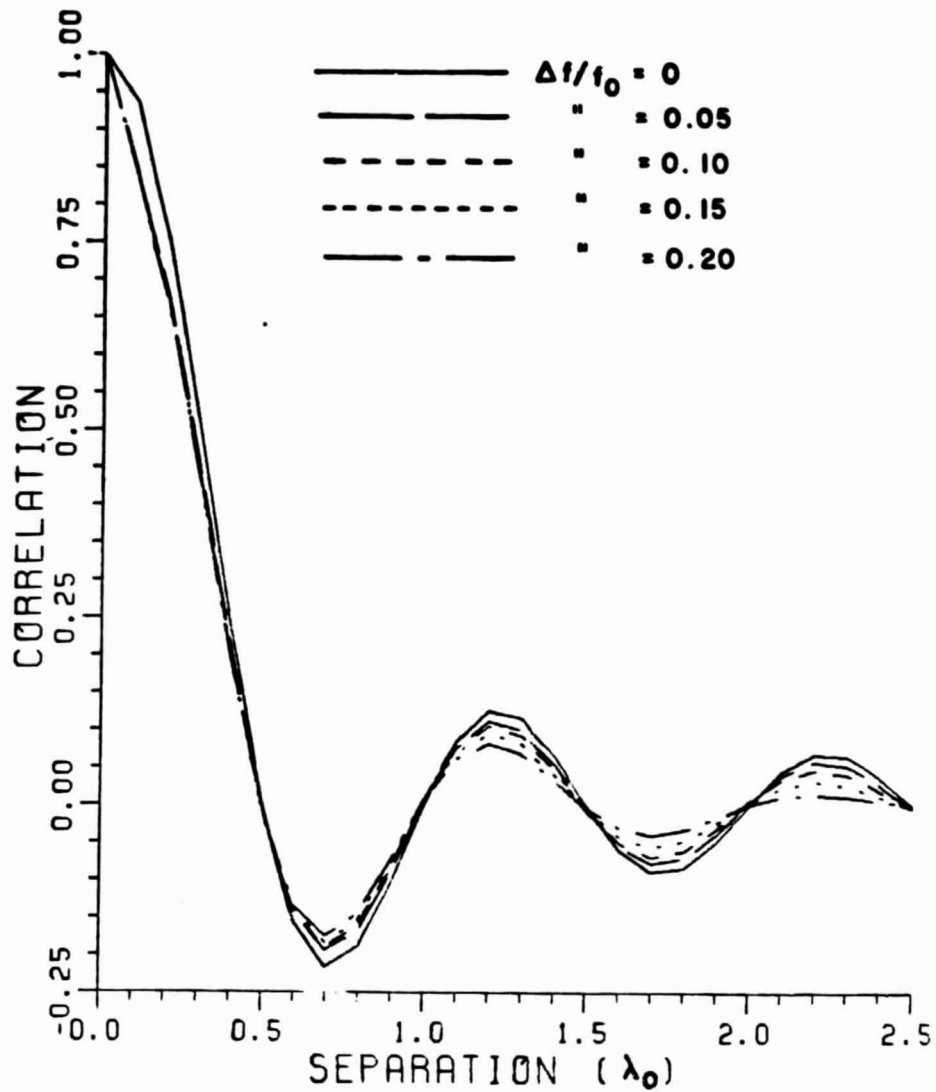


Figure A.4. Noise correlation between two isotropic antennas vs. the separation between antennas for various values of system bandwidth.

if the two antennas are pointed in different directions, the noise entering the two antenna is only partially correlated. The noise correlation decreases with an increase in the angular separation between the main beams of two directive antennas. The noise correlation further decreases with spatial separation between two antennas.

Let the directive antenna be a linear uniform array of N isotropic antennas with interelement spacing of half a wavelength and elements symmetrically distributed along the y axis (Figure A.5). Then the far field of the antenna is given by

$$F(\theta, \phi) = \frac{\sin \left(\frac{N}{2} (\pi \sin \theta \sin \phi + \alpha) \right)}{\sin \left(\frac{\pi \sin \theta \sin \phi + \alpha}{2} \right)} \quad (\text{A.11})$$

where α is the progressive phase shift between the antenna elements to steer its beam in the desired direction. Let

$$\alpha = \pi \sin \phi_0 \quad (\text{A.12})$$

Then

$$F(\theta, \phi) = F(\theta, \phi, \phi_0) = \frac{\sin \left(\frac{N\pi}{2} (\sin \theta \sin \phi + \sin \phi_0) \right)}{\sin \left(\frac{\pi}{2} (\sin \theta \sin \phi + \sin \phi_0) \right)} \quad (\text{A.13})$$

For two such antennas with a separation s wavelengths along the x axis, the noise correlation is given by

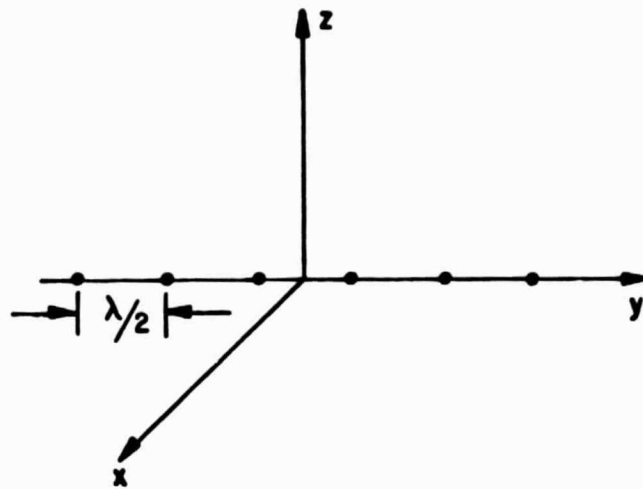


Figure A.5. A linear array of N isotropic antennas.

$$\rho(s, \phi_{01}, \phi_{02}) = \frac{1}{4\pi N^2} \int_0^{2\pi} \int_0^{\pi} F(\theta, \phi, \phi_{01}) \cdot F(\theta, \phi, \phi_{02}) \cdot e^{j2\pi s \sin\theta \cos\phi} \cdot \sin\theta \, d\theta \, d\phi \quad (A.14)$$

where ϕ_{01} and ϕ_{02} are the direction of the main beam of the two antennas in the xy plane. Let $\phi_{01} = -\phi_{02} = \phi_0$. Note that if $\phi_0 = 0$, then the two antennas are steered in the same direction. For other values of ϕ_0 , the two antennas are steered in different directions and the angular separation between the main beams of the two antennas increases with an increase in ϕ_0 .

Using (A.10), the noise correlation between two antennas for various values of ϕ_0 and s is computed and is shown in Figure A.6. In this figure, $N=10$ and ρ is plotted vs. s for various values of ϕ_0 . Note that the noise correlation decreases with an increase in ϕ_0 . The noise correlation also decreases with spatial separation between the two antennas. However, it is more sensitive to ϕ_0 . When ϕ_0 is equal to 5° , the noise correlation is less than 0.15. For a linear array of N isotropic antennas, the half power beam width is approximately equal to

$$\text{HPBW} \approx \frac{57.3^\circ}{L/\lambda} \quad (A.15)$$

where L is the length of the array. In this example

$$L = (N-1) \frac{\lambda}{2} = 4.5\lambda \quad (A.16)$$

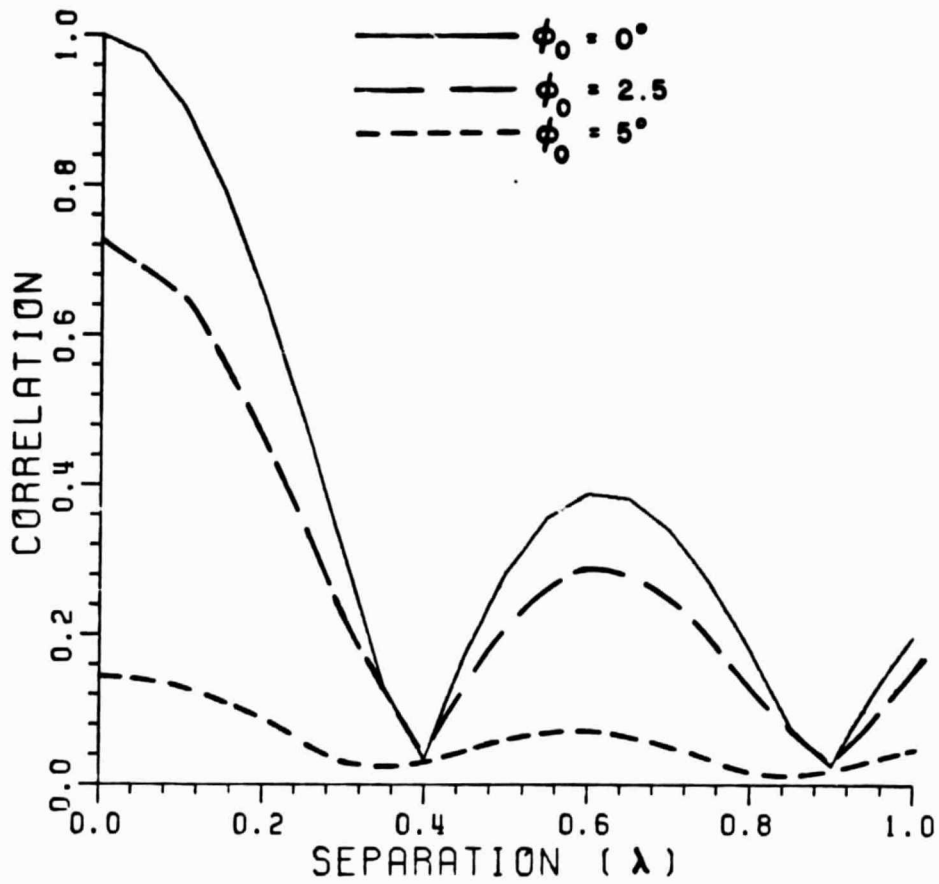


Figure A.6. Noise correlation between two linear arrays of ten isotropic antennas vs. the separation between the two arrays. System bandwidth is assumed to be zero.

Substituting (A.16) in (A.15),

$$\text{HPBW} = \frac{57.3^\circ}{4.5} = 12.73^\circ \quad .$$

Thus, when ϕ_0 is equal to 5° , the angular separation between the main beams of the two antennas is less than their HPBW. Hence, the main beams of the two antennas overlap with each other. If these two antennas are used to receive signals incident along the x axis, the maximum drop in the gain along the signal direction will be less than 3 dB. However, since the noise entering the two antennas arrives from mostly different portions of the observation range, it has relatively small correlation. Thus, in the case of directive antennas, the two antennas may be pointed in different directions to decorrelate the noise without any significant drop in the gain of the antenna in the desired signal direction.